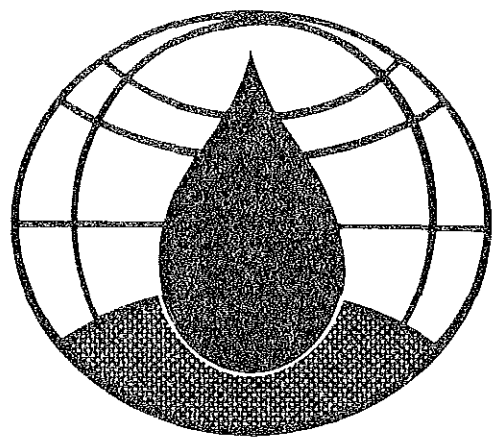


INTERNATIONAL IRRIGATION CENTER



FATE AND TRANSPORT OF TCE-PETROLEUM
HYDROCARBON MIXTURE AT UTR

G. NASH QUASHIGAH
RICHARD C. PERALTA

1992

FATE AND TRANSPORT OF TCE-PETROLEUM
HYDROCARBON MIXTURE AT UTTR

PRESENTED BY:

G. NASH QUASHIGAH (C.E.)

RICHARD C. PERALTA (P.E., PH.D.)

DEPT. OF BIOLOGICAL AND IRRIGATION ENGINEERING

and

INTERNATIONAL IRRIGATION CENTER

UTAH STATE UNIVERSITY

LOGAN, UTAH

SUBMITTED TO:

ENGINEERING SCIENCE, INC.

SALT LAKE CITY, UTAH

and

OFFICE OF ENVIRONMENTAL MANAGEMENT

OOALC/EM

HILL AIR FORCE BASE

OGDEN, UTAH.

REPORT IIC-92/1

FATE AND TRANSPORT OF TCE-PETROLEUM
HYDROCARBON MIXTURE AT UTTR

PRESENTED BY:

G. NASH QUASHIGAH (C.E.)

RICHARD C. PERALTA (P.E., PH.D.)

DEPT. OF BIOLOGICAL AND IRRIGATION ENGINEERING

and

INTERNATIONAL IRRIGATION CENTER

UTAH STATE UNIVERSITY

LOGAN, UTAH

SUBMITTED TO:

ENGINEERING SCIENCE, INC.

SALT LAKE CITY, UTAH

and

OFFICE OF ENVIRONMENTAL MANAGEMENT

OOALC/EM

HILL AIR FORCE BASE

OGDEN, UTAH

REPORT IIC-92/1

TABLE OF CONTENTS

Section

1.0 INTRODUCTION

1.1 Background

1.2 Site Description

1.3 Overview of Chemical Contamination Problem

1.4 Objectives and Scope of Study

1.5 Procedure/Methodology

2.0 STUDY AREA AND CONCEPTUAL MODEL

2.1 Model Parameters and Assumptions:

2.1.1 Geohydrologic Parameters

i. Site geology

ii. Hydrology and Meteorology

2.1.2 Chemical Data and Fluid Properties

2.1.3 Transport Parameters

2.2 Overview of Phase I Simulation and Boundary Conditions

2.3 Overview of Phase II Simulation and Boundary Conditions

3.0 MULTIPHASE FLOW AND MULTICOMPONENT TRANSPORT MODEL

3.1 Numerical Code Description - MOFAT

3.2 Computational Algorithm...

3.3 Model Assumptions

3.4 Code Applicability and Limitations

- 4.0 APPLICATION OF NUMERICAL CODE TO CHEMPIT 4
 - 4.1 Conceptual Model Configuration
 - 4.1.1 Boundary Conditions
 - 4.1.2 Initial Conditions
 - 4.2 Results of Numerical Simulation
 - 4.3 NAPL Infiltration and Redistribution
 - 4.3.1 NAPL Volume
 - 4.3.2 Bulk Fluid Viscosity
 - 4.3.3 Bulk Fluid Density
 - 4.3.4 Bulk Fluid Flux
 - 4.3.5 Soil Permeability
 - 4.4 Partitionable TCE Transport
 - 4.4.1 Media Dispersivity
 - 4.4.2 Soil Adsorption
- 5.0 SUMMARY OF ACCOMPLISHMENTS
- 6.0 CONCLUSIONS
- 7.0 RECOMMENDATIONS
- 8.0 ACKNOWLEDGEMENTS
- 9.0 REFERENCES
- 10.0 FIGURES

LIST OF FIGURES

- Figure 1.2 Location of sites at UTTR North Range, Utah
- Figure 1.3 Areal extent of chemical contamination at Chempit 4
- Figure 2.1.1a Actual geologic cross section at Chempit 4
- Figure 2.1.1b Cross-section of idealized geology of Chempit 4 used for modelling.
- Figure 4.1a Problem description and boundary conditions: Oil-TCE mixture infiltration phase (phase I)
- Figure 4.1b Problem description and boundary conditions: NAPL redistribution and partitionable TCE transport phase (phase II)
- Figure 4.3.1a NAPL Saturation Contours: (Input NAPL volume equals 250,000 gallons)
- Figure 4.3.1b NAPL Saturation Contours: (Input NAPL volume equals 500,000 gallons)
- Figure 4.4a P-phase concentration distribution of TCE after 5 years of phase II
- Figure 4.4b P-phase concentration distribution of TCE after 10 years of phase II
- Figure 4.4c P-phase concentration distribution of TCE after 14 years of phase II
- Figure 4.4d P-phase concentration distribution of TCE after 25 years of phase II
- Figure 4.4.1 Effect of dispersivity on water phase TCE concentrations after 5 and 14 years of phase II

Figure 4.4.2 Effect of adsorption on TCE concentrations after 14 years of phase II

1.1. Background

In 1988 a preliminary assessment (PA) study was conducted at Chemical Disposal Pit No. 4 to address several concerns of Hill Air Force Base (HAFB), the facility operators. The objectives of the PA were; i) to assess the potential for organic chemical releases to the subsurface environment, and ii) to determine the need for any immediate control measures, if the subsurface environment were threatened.

It was concluded from the PA that the potential for vadose zone contamination at Chempit 4 might be high. However, the threat to groundwater, in particular Wells 1 and 2 which provide drinking water for the Oasis complex personnel was considered minimal. Consequently, it was recommended that field investigations be conducted to collect soil samples and geologic data to adequately delineate the problem. The conclusions drawn from the PA were based on the following factors.

- . Low annual precipitation at the site (less than 10 inches per year)
- . High potential evapotranspiration (ETP) rate (83 in/year)
- . Low vertical soil permeability, which might suggest a limited potential for groundwater contamination.
- . Chempit 4 is located downgradient (1.5 miles) from drinking water Wells 1 and 2
- . None of the high mobility chemical constituents of the disposed liquid waste, such as trichloroethylene, were

detected in wells number 1 and 2.

- . Groundwater flow is expected to be in a direction away from the potable water wells.

In 1989 HAFB implemented the recommendations of the PA study by awarding a contract to Engineering Science, Inc., to collect contaminated soil samples at Chempit Disposal Pit No. 4. The samples were to be used for geotechnical and chemical analysis.

1.2 Site Description

Chemical Disposal Pit No. 4 henceforth termed "Chempit 4", is an abandoned waste disposal facility that was used for the disposal of industrial waste generated at HAFB. Chempit 4 is part of a larger gravel pit located approximately 1.5 miles northwest of the UTTR personnel complex. Chempit 4 measures 15 feet by 20 feet and is 8 feet deep. Figure 1.2 shows the location of Chempit 4 within UTTR North Range, Utah.

1.3 Overview of Chemical Contamination Problem

Between 1973-1975 approximately 500,000 gallons of industrial liquid wastes generated at HAFB were disposed of into Chempit 4. Although, we lack documentation on the actual composition and total volume of the waste, available information suggests an approximate disposal rate of roughly 20,000 gallons per month. The wastes consisted primarily of nonaqueous phase liquids (NAPL).

UTTR personnel strongly believe that the NAPL consisted primarily of waste engine oil and small quantities of diesel fuel

and degreasing organic solvents/chemical solvents. Figure 1.3 shows the areal extent of chemical contamination at Chempit 4, which for all practical purposes had been abandoned since 1975.

1.4 Objectives of the Study

The primary objectives of this study are two-fold. The first objective is to model the infiltration and redistribution of an OIL-TCE mixture (NAPL) through the unsaturated zone of Chempit 4.

The second major objective is to predict the fate and transport of partitionable TCE in the aqueous and soil phases.

To accomplish the proposed objectives, a number of numerical simulations were performed. Some simulations predicted the migration and resulting areal extent of NAPL contamination. Others predicted the transport of partitionable TCE to determine if groundwater quality will be threatened.

1.5 Procedure/Methodology.

A comprehensive methodology for predicting the transport and fate of nonaqueous phase liquids is developed and applied to the uncontrolled migration of Oil-TCE mixture through the unsaturated zone at Chempit 4. The proposed methodology relies on a comprehensive three-phase flow, multicomponent transport finite element model (ESTI, 1990). In applying MOFAT to Chempit 4, the model's salient features were combined with some innovative modeling approaches to i) determine model input parameters, ii)

minimize the number of assumptions employed compared to traditional multiphase flow models, iii) optimize the computational efficiency of the model, and iv) improve the accuracy of the predicted solutions.

The methodology developed to accomplish the project's goals included the following steps;

a) develop conceptual model and boundary conditions describing the problem, b) estimate all unknown multiphase flow and transport input data, e.g composition of fluid mixture, volume of infiltration, aquifer dispersivity, adsorption coefficients etc. c) calibrate model to simulate NAPL infiltration, d) calibrate model to simulate NAPL re-distribution and TCE transport, and e) predict future NAPL migration and TCE transport in the vadose zone. Sensitivity analyses was performed during several of the above steps.

Mathematical and physical constraints of the applied model and fluid properties dictate that numerical simulations be performed in two separate stages, namely phase I and phase II simulations.

Phase I simulations model the infiltration of NAPL through the upper soil profile of Chempit 4. The duration of this phase is two years and defined as the time period from initiation to the termination of NAPL disposal activities at Chempit 4 (1973-1975). Partitionable TCE transport is neglected during this phase for the following reasons a) numerical instability of computed solutions resulting from initially high NAPL velocities were observed, and b) it was assumed that mass transfer during this relatively short

period will not significantly affect computed solutions because of low NAPL solubility.

Phase II simulations model NAPL re-distribution and noninert/partitionable TCE transport through the subsurface system (1975-1989). Sensitivity analyses and model calibration were performed in both phases I and II.

2.0 STUDY AREA AND CONCEPTUAL MODEL

2.1 Model Parameters and Assumptions

The conceptual model describing NAPL contamination at Chempit 4 consists of a waste disposal pit leaking a multicomponent liquid waste into a thick stratified unsaturated zone.

To adequately model NAPL migration at Chempit 4, site specific input variables including geohydrologic properties, boundary conditions, fluid properties, transport parameters, and other model parameters must either be known a priori, measured in the field, determined from laboratory data, or obtained from literature.

Data collected from a recent Chempit 4 site inspection (SAIC, 1990) does not provide sufficiently detailed information for a modeling study. As a result, literature values or Landfill 5 data were utilized when necessary.

2.1.1 Geohydrologic Parameters

i. Site geology

In the present study, the conceptualized geology of Chempit 4 is derived from field data. Some site details can be found in the site inspection report (SAIC, 1990). Figure 2.1.1a is a cross-section through two soil borings (SB-01 and SB-02) showing the different soil layers that constitute the stratigraphy. Some assumed values are included.

Although the two borings are only 50 feet apart, the upper 45-60 feet of soil profile exhibit a different genesis at the two

locations. That is, while the top 35 feet of deep boring (SB-01) contains a 10-foot layer of coarse gravel below a 25 foot layer of silt, the top 35 feet of the shallow boring (SB-02) contains a 25-foot layer of sand and gravel, sandwiched between two 5-foot layers of silt. Complicating estimation of the appropriate geology for the conceptual model was the absence of measured soil properties below 65 feet and 35 feet for SB-01 and SB-02 respectively.

For SB-02, we assumed the soil properties of SB-01 from depths of 35 to 90 feet.

For conceptual and modelling purposes, the soil zones were then formed into two idealized zones (Fig. 2.1.1b). The hydraulic conductivity of these zones were harmonic means of the previously observed and assumed data of SB-01. This was done for the following reasons:

a) There was lack of sufficient geologic data needed to perform a comprehensive evaluation of soil spatial variability effects.

b) It was necessary to minimize numerical instability of predicted solutions.

The lower 90-foot layer of the conceptual model was assumed to be a homogeneous mix of gravelly sand and sandy gravel.

ii. Hydrology and Meteorology

Groundwater elevations at Chempit 4 were not measured. However, it was inferred from Landfill-5 and Wells 1 and 2 that the water table at Chempit 4 is approximately 150 ft below the soil

surface (4216 feet above MSL). Regional groundwater flow is towards the northwest (i.e towards the Great Salt Flats). The climate of the site is arid, with annual precipitation of 10 inches or less. Potential evapotranspiration is much greater than 10 in/yr. Precipitation occurs primarily from November through February.

2.1.2 Chemical Data and Fluid Properties

No records were kept on the volume and composition of the liquid waste disposed into Chempit 4. UTTR complex personnel suggest the facility may have received approximately 500,000 gallons of industrial waste composed primarily of waste engine oil with small quantities diesel fuel and chemical solvents.

As part of a Chempit 4 site inspection plan, a soil gas analysis was performed by TRC under the supervision of SAIC personnel. The primary objective of the investigation was to identify the volatile organic constituents (VOCs) of the NAPL present at the site. The ideal locations for future soil borings were identified as being those areas showing the highest concentrations of soil gas. Soil samples from the borings were used for geologic and chemical analysis. Eleven (11) VOCs were selected as target analytes for the purpose of soil gas analysis. These include BTEX (benzene, toluene, ethylbenzene, and xylene), total hydrocarbons, trichlorotrifluorethane, 1,1 -Dichloroethane (1,1 -DCE), 1,2 -trans dichloroethylene (DCE), trichloroethane (TCA), tetrachloroethylene (PCE), and Trichloroethylene (TCE).

Chemical analysis of the contaminated soil samples showed high adsorbed phase concentrations of volatile organic compounds (VOCs) and SVOCs (45,000 ug/kg of TCE, 78,000 ug/kg for BTEX compounds, and 496,000 ug/kg of tentatively identified compounds (TICs). The highest level of adsorbed concentration at Chempit 4, 14,000 mg/kg, was measured for total petroleum hydrocarbons (TPH).

Chemical analysis of the contaminated soil samples indicate the presence of metals, volatile (VOCs) and semi-volatile (SVOCs) compounds. The metals include aluminum, iron, lead, nickel, barium, and others. These could be impurities from engine operation. Identified VOCs include trichloroethylene (TCE), tetrachloroethylene (PCE), 1,1-Dichloroethane, Benzene, Toluene, Ethyl benzene, Xylene, among others. The SVOCs include polycyclic aromatic compounds (PAHs) such as Naphthalene, Fluorene, Anthracene, Pyrene, Phenanthrene, among others. PAHs and BTEX compounds are major constituents of mineral based crankcase oil, and diesel fuels. In the absence of measured chemical properties, literature values of the waste liquid were used in the present study.

The bulk fluid properties which are input to the numerical model, MOFAT, are the capillary pressure curve scaling parameters, fluid densities, fluid viscosities, and mass fraction of fluid components. Procedures for calculating these properties are outlined in the MOFAT program documentation (ESTI, 1990).

2.1.3 Transport Parameters

Aside from bulk fluid properties, individual component properties needed to model the multiphase flow and partitionable component transport include the diffusion coefficients in bulk water, oil, and air, the oil-water, air-water, and soil-water partition coefficients, and the first order decay coefficients.

Molecular diffusion coefficients of industrial chemicals (e.g TCE) in bulk water or air can be estimated from semi-empirical methods (Lyman et al., 1982), or may be found in literature. An empirical statement relating bulk oil diffusion coefficients water phase diffusion coefficients is given by ESTI (1990).

2.2 Overview of Phase I Simulation

Phase I simulations model the infiltration and distribution of NAPL through the unsaturated zone of Chempit 4. As discussed earlier, the maximum allowable volume of NAPL infiltration was chosen as 500,000 gallons. The infiltration period was two (2) years, defined as the time period from initiation to termination of NAPL disposal activities at chempit 4. Transport of the target partitionable component i.e noninert TCE during the infiltration phase is neglected due to the following reasons:

- . Mass transfer rates and changes in fluid properties for low solubility compounds over short time periods might be small. Simulations involving negligible deep percolation rates may validate this assumption.

- . Due to model constraints and general complexity of the

coupled, nonlinear multiphase flow and multi-component transport equations, numerical instability was encountered during initial periods of high NAPL flow.

. Neglecting partitionable TCE transport during NAPL infiltration phase, reduces phase I computational effort without significant loss of numerical accuracy during phase II simulations.

. Because changes in fluid properties during Phase I are assumed small, preliminary sensitivity analysis on fluid (viscosity, density, etc) and hydrogeologic (soil permeability, porosity, etc) properties are performed during phase I.

Results of numerical simulations by Parker et al.(1988) also indicate that mass transfer rates and fluid density updating have negligible effects on predicted solutions during periods of highly transient NAPL flow.

Output from Phase I simulations include, distribution of NAPL and water hydraulic heads, and the distribution of NAPL, water and air saturations.

2.3 Overview of Phase II Simulations

Phase II simulations commence after a specified volume of NAPL infiltrates the unsaturated zone of Chempit 4. Phase II simulations predict NAPL re-distribution and partitionable Tce transport. Both fluid flow and component transport equations are solved during this phase. Thus computational effort is more expensive and time consuming than phase I simulations. A number of simulations were performed during phase II to accomplish the following the

objectives:

a) calibrate (to available field data) NAPL contamination in terms of lateral spreading, vertical extent of movement, and location of maximum NAPL saturation contour within the contaminated soil profile.

b) calibrate (to available field data) adsorbed TCE concentrations within the contaminated soil profile.

c) perform sensitivity analysis on model input parameters, to determine changes in numerical solutions in response to variations in input parameters.

d) predict future NAPL migration and TCE transport through the vadose zone.

Simulations in this phase begin after phase I terminates. Thus, a ten year phase II simulation predicts values 12 years after infiltration begins (2 + 10 years).

3.0 MULTIPHASE FLOW AND MULTICOMPONENT TRANSPORT MODEL

3.1 Description of Numerical Code: MOFAT

MOFAT is a 2-dimensional cross-sectional or radially symmetrical finite element model for simulating nonlinear, coupled multiphase flow and multicomponent transport under saturated-unsaturated conditions. The flow module can be used to simulate the behavior of an organic chemical that may exist in three distinct phases, i) immiscible nonaqueous phase liquid (NAPL), ii) water, and iii) dynamic or static gas phase. The transport module can accommodate up to 5 noninert components which may partition into the aqueous, soil or gas phases under the assumption of local equilibrium interphase mass transfer.

Gas phase volatilization and/or water phase evaporation from the ground surface is not considered in the transport module.

The input data required for the flow simulation consist of boundary and initial conditions, fluid properties, soil hydraulic properties, solution stability factors (upstream weighting factor), time integration parameters, and mesh geometry. A modified Van Genuchten model which accounts for oil entrapment during periods of water imbibition is used to define three phase permeability-saturation-capillary pressure relations. The flow module can handle stratified soils with up to 10 different soil layers. The transport module requires additional input data such as porous media dispersivity, equilibrium partition coefficients, diffusion coefficients, first order decay coefficients, component densities

and boundary and initial conditions.

3.2 Computational Algorithm:

The governing equations consist of the nonlinear, coupled multiphase flow equations for NAPL, water and gas phases and the multicomponent transport equations of partitionable NAPL components. The nonlinearity of the flow equations results from the functional dependence of phase permeability on a primary variable, (e.g phase saturation). The flow equations are coupled due to the functional relationship between fluid saturations, permeabilities, and pressures.

Coupling of the flow and transport equations occurs through the interphase mass transfer terms and through the inter-dependence of scaling factors, phase density, phase viscosity and other flow and transport coefficients. The interaction between flow and transport dictates the flow equation be solved simultaneously with or prior to evaluating the transport equations.

For low solubility organic fluids, changes in fluid properties resulting from phase partitioning (mass transfer) over short time periods will be small (ESTI, 1990). Consequently, for short flow times the flow and transport equations can be decoupled and solved serially. For very large simulation periods, however, dissolution and volatilization are expected to be significant. Since these processes will affect fluid composition and fluid properties, mass transfer rates are best continuously updated to account for these changes.

The flow and transport equations are directly coupled via fluid velocity and phase saturation, and coupled in the functional form through the transport dispersion coefficients. However, the weak coupling between the two equations permits one to solve the transport equations serially with the flow equations. Furthermore, assuming negligible interactions between individual fluid components leads to a weak coupling between the individual component transport equations. Thus, the transport equation for the different components may be solved serially in any sequence.

A complete description of the governing equations, and the finite element formulations can be found in the MOFAT documentation (ESTI, 1990). A summary of the basic solution approach employed by MOFAT is presented:

1. Solve the fluid flow equations simultaneously for the current time step using time lagged phase densities and interphase mass transfer rates.
2. Solve the phase summed transport equations using time lagged phase densities and interphase mass transfer rates.
3. Back-calculate new interphase mass transfer rates and update phase densities for the current time step.
4. Proceed to the next time step.

3.3 Model Assumptions

MOFAT is a comprehensive multiphase flow and multicomponent transport model formulated to minimize the number of assumptions

associated with traditional multiphase flow models.

For example, while many multiphase flow models neglect the gas flow equation by assuming negligible gas pressure gradients, MOFAT provides the option of simulating a static or dynamic gas phase.

Nevertheless, as with any mathematical model, some assumptions were made to formulate the governing equations. Some of these assumptions include:

- . Bulk fluid density and viscosity are pressure independent, but vary in time depending on the mass of each component entering or leaving the phase.
- . A modified Van Genuchten model defines the three phase permeability-saturation-capillary pressure relations.
- . Soil porosity is independent of bulk fluid pressure
- . Darcy's law is valid for multiphase flow.
- . Flow is in a porous media
- . Organic constituents can partition between the nonaqueous liquid, water, gas and solid phases under the assumption of local chemical equilibrium.
 - a) NAPL-WATER partitioning is described by the equilibrium solubility approach.
 - b) Henry's law describes AIR-WATER partitioning
 - c) SOLID-WATER partitioning is described by a linear, reversible, equilibrium isotherm.
- . Decay of the organic chemical occurs exclusively within the aqueous phase, thus decay coefficients in the nonaqueous and air phases are ignored

3.4 Code Applicability and Limitation

MOFAT can be applied to simulate multiphase flow and multicomponent transport of an organic chemical through deep or shallow aquifers and under saturated and unsaturated conditions. It is especially useful for modeling the migration of industrial wastes consisting of five (5) or less partitionable components. The code will accommodate a heterogeneous soil system consisting of at most 10 different soil layers.

The code can also be used to formulate, and analyze the effect of remedial technologies at hazardous waste sites, or to pursue the cleanup and remediation of chemical spills, leaks from surface impoundments, or infiltration from waste disposal facilities. The code can be applied to many practical problems, however, it has three primary limitations: i) inability to simulate volatilization of organic chemicals from the soil surface, ii) inability to simulate evaporation of soil moisture from the soil surface, and iii) excessive computational cost for large solution domains.

4.0 APPLICATION OF NUMERICAL CODE TO CHEMPIT 4

4.1. Conceptual Model Configuration

In evaluating the applicability and efficiency of MOFAT to subsurface contamination problems, the code was applied to simulate the migration of a TCE-hydrocarbon fuel mixture through the unsaturated zone of Chempit 4. Figures 4.1a and 4.1b show the description of the conceptual model and boundary conditions. The model domain is 200 feet wide and 150 feet deep. The conceptual soil profile consists of a 90-foot layer of sandy gravelly soil overlain by a 60 foot layer of silty soil.

4.1.1 Boundary Conditions:

Figure 4.1a depicts the idealized NAPL infiltration at Chempit 4, i.e Phase I simulations. There, Q_o and Q_w represent flow of oil and water respectively. Q^* is an assumed application rate. H , H_1 and h_w represent the elevation (head) of the water table, q_n^* is deeply percolating precipitation, (assumed zero in phase II simulations). C_{aw} is the aqueous phase concentration. The idealized domain is assumed initially free of organic chemicals. Then NAPL is allowed to infiltrate the vadose zone through a 20 foot long source at the soil surface. Specified volumes of the NAPL were allowed to infiltrate continuously for a two year period. Infiltration was terminated thereafter. The boundary conditions for the NAPL are all no flow boundaries, except at the source where a known flux boundary condition was specified. For water, no flow

boundary conditions along the left, right and upper boundaries, and a constant head boundary at the lower boundary (water table) was specified.

Figure 4.1b also depicts the idealized system and boundary conditions during NAPL re-distribution and partitionable TCE transport, i.e Phase II simulations. Boundary conditions for water are unchanged, and NAPL is subject to no flow boundary conditions on all boundaries. For partitionable TCE transport, a zero concentration gradient was specified on the left, right and lower boundaries. This boundary condition specifies a zero normal dispersive flux since it was assumed no flow occurs through the boundaries. A zero concentration gradient was also imposed on the upper boundary to simulate a zero mass flux condition.

In some sensitivity runs/simulations, constant water head boundary condition were imposed along the left and right boundaries. These simulations were performed to examine the effect of boundary conditions on NAPL and partitionable TCE behavior.

4.1.2 Initial Conditions:

General mathematical expressions for flow initial conditions stipulate fluid pressures at all nodes in the domain (ESTI, 1990). Fluid pressure heads in the flow domain above the water table are computed according to the relations:

$$h_w = a + bz, \quad h_o = c + dz$$

Here, z is the elevation along the vertical transect of the boundary, and a, b, c and d are input variables (ESTI, 1990). Under

equilibrium conditions, $a = z_{aw}$, $b = -1$, where z_{aw} is the air-water table elevation, or defines the point in domain where water pressure head, $h_w = 0$. The other input variables are defined the MOFAT documentation (ESTI, 1990).

For partitionable TCE transport, the initial conditions are stated in terms of water phase concentration. Zero aqueous phase concentrations were input to all uncontaminated points while initial water phase concentrations of TCE were assigned to contaminated points in the modeled domain.

4.2 Results of Numerical Simulations

Inadequate data regarding geohydrologic and fluid properties at Chempit 4 made it difficult to quantify these parameters. Field data indicate that soil hydraulic properties can have wide spatial variability. The actual composition of the organic chemical is also unknown, and laboratory measurements of fluid properties such fluid viscosity and density are lacking.

To investigate the effect of uncertainty and variation of input parameters on predicted solutions and to validate selected base input data, several numerical simulations were performed. These simulations, which included calibration and sensitivity analysis, were performed by 1) varying the magnitude of the input parameters across a range of likely values 2) matching numerical results to field data and 3) observing the parameters which exert controlling effect on computed solutions.

The input parameters chosen for extensive analyses of NAPL and

partitionable TCE behavior in this study include the following:

fluid parameters

bulk fluid density (fluid composition)

bulk fluid viscosity

NAPL flux rate

volume of NAPL infiltrated

geohydrologic parameters

permeability of porous media

media porosity

permeability-saturation-capillary pressure functions

transport parameters

mass transfer coefficients

porous media dispersivity

organic carbon content (adsorption coefficients)

initial concentrations of TCE

diffusion coefficients

4.3 NAPL Infiltration and Redistribution

4.3.1 NAPL Volume

Figures 4.3.1a and 4.3.1b depict NAPL migration through the vadose zone of Chempit 4. Several numerical simulations were performed to examine the effect of critical fluid flow parameters on NAPL behavior. However, general NAPL infiltration and redistribution dynamics at Chempit 4 will be described with the aid of these two figures. The white line running from the left to right

boundary in these figures mark the border of the upper and lower soil layers of the conceptualized model.

Since the actual volume of NAPL that infiltrated into Chempit was unknown, NAPL volume was varied across a range of probable values to reflect the uncertainty in that parameter. To account for NAPL lost to volatilization and other biochemical processes, several numerical simulations involving i) a base value of 500,000 gallons, ii) 75 percent of the base value (375,000 gallons), iii) 50 percent of base value (250,000 gallons), and iv) 25 percent of base value (125,000 gallons) were performed.

It was apparent from the simulations that the areal extent of contamination, (i.e lateral spreading and depth of penetration) varied with the magnitude of NAPL infiltration volume. Because gravity flow was the predominant driving force during the redistribution period, downward movement was greater than lateral spreading.

Assuming a 500,000 gallons infiltration volume, NAPL would reach the vicinity of a water table located 150 feet (45m) below the ground surface (figure 4.1.1d), fourteen years (i.e 1975-1989) after NAPL infiltration ceases. There would still be localized patches of NAPL saturations exceeding the residual level ($S_r = 0.2$). Further downward migration would be possible. Thus over a given time period NAPL may reach the groundwater.

Using infiltration volumes of 375,000 gallons and 125,000 gallons yielded solutions which deviated from field data. Field data indicate a contaminated areal extent which measures 100 feet

(30.5m) laterally and 64 feet (19.5m) deep. Simulations using a NAPL volume of 250,000 gallons compared favorably to field data and thereby chosen as the "ideal" (assumed) NAPL volume.

NAPL migration, described by NAPL saturation contours for the 250,000 gallon NAPL volume, is shown in Figure 4.3.1a. Fourteen years after NAPL infiltration ceases (i.e. 1989) a symmetrical areal contamination, about 100 feet wide and 65 feet has developed. In fact, little or negligible downward NAPL movement is observed after the the fifth year of re-distribution (Figure 4.3.1a). After fourteen years of infiltraton the highest NAPL saturation is 0.42. Located in what is termed the core saturation, it is shown by the brown contour in Figure 4.3.1b. This zone is located directly below the source at a depth of 23-35 feet (7-11 meters). The saturation profile defined as the areal extent of NAPL core/maximum saturation compares favorably with observed profile of the deep soil boring (SB-01) (Figure 1.3 and Engineering Science, 1989, pg 4-37). Consequently, it is concluded that 250,000 gallons of the total applied NAPL volume infiltrates the unsaturated zone and the rest was lost to volatilization and other biochemical processes. This is easily justified since the initially assumed 500,000 gallons could have been overestimated.

4.3.2 Bulk Fluid viscosity:

The behavior of high and low viscosity NAPLs was significantly different throughout the simulations. To demonstrate the effect of fluid viscosity on NAPL mobility, the base fluid viscosity of 2

centipoise (cP) was more than doubled to 5cP in one sensitivity study, and decreased by 50 percent in another simulation. These viscosity values were chosen to reflect the wide variation in bulk fluid properties (Oak Ridge, 1989).

The low viscosity NAPL was observed to move quickly and penetrate the aquifer to a greater depth. Lateral spreading from the source in both positive (+) and negative (-) x direction was limited, however. Conversely, the more viscous NAPL penetrated the vadose zone to a shallower depth, but did spread laterally beyond the observed contamination zone.

4.3.3 Bulk Fluid Density:

Density effects were examined by simulating the migration of low density (i.e. % TCE equal 2.5%) and high density (i.e. % TCE equal 5%) NAPLs. Model predictions show that the light NAPLs were immobilized in the upper unsaturated zone, however lateral spreading was significant.

Gravity effects were dominant in dense NAPL simulations. NAPL migration was primarily downward with relatively small lateral spreading. The practical implication of these results is that dense, low viscosity NAPL poses a greater threat to subsurface resources because it can travel deeper and faster.

4.3.4 Bulk Fluid Flux

To minimize the potential for NAPL pressure buildup on the

soil surface, the maximum NAPL flux rate used in the sensitivity study was chosen to equal the prevailing medium permeability. The effect of increasing NAPL flux rate is similar to increasing fluid viscosity in that both increase lateral spreading, (Kaluarachchi and Parker, 1988).

4.3.5 Soil Permeability

The behavior of NAPL in response to variations in soil permeability was similar to NAPL migration patterns under varying fluid viscosity conditions. In this analysis, the permeability of the upper hydraulic zone was varied by 2 orders of magnitude. i.e 10,000 percent to reflect parameter uncertainty. As previously discussed, the upper zone, which naturally consists of 5 geologic units is represented in the conceptual model by a single hydraulic unit with permeability equal to the harmonic mean of those 5 units. Thus maximum and minimum vertical permeabilities of the conceptualized upper soil layer, depicted in Figure 2.1.1a, are 0.864 m/d (permeability of coarse sandy gravel) and 0.0023 m/d (permeability of fine silty sand) respectively.

It was evident from computed solutions that as the vertical permeability of the upper geologic unit was decreased, vertical movement of the NAPL was restricted while lateral spreading increased. In the absence of significant inhomogeneity, numerical simulations show that NAPL migration is primarily downward in moderate to highly permeable soils.

The effect of three phase permeability-saturation-capillary

pressure relationships on computed solutions could not be explicitly evaluated because it was input to the model as a function. The Kr-S-Pc relationship are unique to a given soil and are site specific. These relationships must be determined for a given site. Because complete data needed to derive the Kr-S-Pc function for Chempit 4 was missing, literature values for soils with similar characteristics to Chempit 4 soils were used (Table 4-1). The sensitivity to variations in porous media porosity was small.

Table 4-1

Typical Soil Properties for Various Soil Types (ESTI,1990)

| Soil type | K_{swz} (m/d) | ϕ (-) | S_m (-) | α (m^{-1}) | n (-) |
|-----------------|--------------------|---------------|--------------|--------------------------|------------|
| Sand | 7.1 | 0.43 | 0.09 | 14.5 | 2.7 |
| Loamy sand | 3.5 | 0.41 | 0.15 | 12.4 | 2.3 |
| Sandy loam | 1.06 | 0.41 | 0.15 | 7.50 | 1.9 |
| Sandy clay loam | 0.31 | 0.39 | 0.26 | 5.9 | 1.5 |
| Loam | 0.25 | 0.43 | 0.19 | 3.6 | 1.6 |
| Silty loam | 0.11 | 0.45 | 0.16 | 2.0 | 1.4 |
| Clay loam | 0.062 | 0.41 | 0.22 | 1.9 | 1.3 |
| Silt | 0.060 | 0.43 | 0.07 | 1.6 | 1.4 |
| Sandy clay | 0.029 | 0.38 | 0.26 | 2.7 | 1.2 |
| Silty clay loam | 0.107 | 0.43 | 0.21 | 1.0 | 1.2 |
| Silty clay | 0.0048 | 0.36 | 0.19 | 0.5 | 1.1 |

4.4 Partitionable TCE Transport

Generating a colored diagram which differentiates the various

isoclors (concentration contours) of partitionable TCE involves some loss of clarity in the diagrams. Despite this, it is necessary to employ such figures in presenting simulation results.

The transport of TCE in the aqueous, adsorbed and gas phases through the vadose zone of Chempit 4 is depicted in Figures 4.4a-d. The figures show the distribution of TCE concentration after four different simulation periods, 5, 10, 14, and 25 years respectively. The units of concentration are parts per million (ppm) for water and gas phase concentrations, and milligrams per kilogram (mg/kg) for the soil phase. In p-phase, "p" denotes air, water or gas.

An intent of this study is to track the transport of partitionable TCE through the vadose zone to determine the potential for groundwater contamination from each partitionable phase. Using the drinking water standard of TCE, 5 parts per billion (5ppb or 0.005ppm) as the "critical concentration", the movement of the 5ppb isochlor is tracked in time until it reaches the water table.

In Figure 4.4a the 5ppb water phase concentration (at its deepest location) is 5 meters above the water table after a 5 year transport simulation period. This implies that only 5 years after NAPL redistribution ends and TCE transport begins, soluble TCE is already near the vicinity of the water table. Soil and gas phase concentrations for the five (5) year time period are also depicted in Figure 4.4a.

A plot of the ten (10) year simulation period (Figure 4.4b)

shows that the 5ppb isochlor reached the water table within 10 years. Figure 4.4c shows the p-phase concentration distribution of TCE for a fourteen (14) year simulation period. The 5 ppb water phase isochlor has already reached the water table and is not visible in the plot.

Figure 4.4d depicts predicted TCE transport through the vadose zone. The simulation period is 25 years.

The effect of input data on TCE partitioning into the water, gas and soil phases and subsequent TCE migration was extensively investigated. However, only the parameters determined as important variables in delineating our findings are presented herein.

4.4.1 Media dispersivity

Porous media dispersivity values were unavailable for Chempit 4. The dispersivity of an aquifer material is site specific and depends on numerous physical variables. Acquiring laboratory or field data concerning this variable is time consuming and cost prohibitive. A number of simulations were performed using varying longitudinal (α_l) and transversal (α_t) values to evaluate their effect on TCE behavior. The dispersivity values were varied across a given range determined from numerical criteria or recommended from literature.

The mesh Peclet number (Pe_m) is a numerical criteria defined as the ratio of element mesh size to longitudinal dispersivity.

$$Pe_m \approx \frac{\max |\Delta x, \Delta z|}{\alpha_l} \leq 2$$

This criterion is used to estimate the maximum element mesh size (given a porous medium dispersivity) necessary to preserve stability of the predicted solutions. Violations of the Peclet number criteria often leads to unstable solutions because the solute transport equation assumes a hyperbolic character. This happens when advection becomes the predominant transport mechanism.

Due to the excessive computing effort involved in running MOFAT, and the lack of measured dispersivity values, the simulated domain was discretized to obtain the fewest number of elements. Using a mesh Peclet number criteria, ($Pe_m \leq 2.0$), and the discretized element mesh, dispersivity values were computed. These dispersivity values were then used in the numerical simulations to determine the effect of dispersivity on TCE transport.

The mesh Peclet criteria, $Pe_m \leq 2$, was chosen after preliminary runs indicated that a mesh Peclet number exceeding 2.0 sometimes yields erroneous results.

Results of the analysis indicated that aquifer dispersivity had negligible influence of TCE processes. Further analysis of dispersivity effects revealed that p-phase velocities of TCE were relatively small, hence low solute dispersion and advection resulted.

In another attempt to evaluate the effect of dispersivity on TCE transport behavior, aquifer dispersivity was estimated as 5 percent of the maximum of the lateral and vertical extent of contaminated soil (ESTI, 1990). From Chempit 4 data, the estimated aquifer dispersivity value was 1.5m. Using the mesh Peclet

criterion of 2.0, results in a maximum element mesh size of 3.0m.

Simulations were run using dispersivities of 4 and 2 (corresponding to Peclet numbers of 1 and 2, respectively). These produced solutions which further confirmed the assumption that aquifer dispersivity had a negligible effect on TCE behavior (Figure 4.4.1).

4.4.2 Soil Adsorption

The mobility of TCE in the subsurface environment is inversely related to the organic carbon content of the soil. Schwarzenbach and Westhall (1981) determined from laboratory sorption studies that over 85 percent of sorption by aquifer materials occurs at particle sizes smaller than 0.125mm for halogenated organic compounds and other non-polar organic compounds. TCE is highly mobile in soils with low organic carbon and vice versa. Chempit 4 is composed predominantly of fine silty sand to coarse silt in the upper 60 feet (18.3m) of top soil. The lower stratigraphy is composed of coarse gravelly sand. Mechanical sieve analysis of soil samples taken from the upper 60 feet of the unsaturated zone indicate that 10 to 60 percent of the soil particles were smaller than 0.10mm.

Results of numerical simulations suggest that adsorption strongly influenced TCE migration by retarding its lateral and vertical advance through the vadose zone. Figure 4.4.2 depicts the effect of adsorption on TCE transport. Using an organic carbon fraction of 10 percent (compared to base value of 1.0 percent for

Chemplot 4) shows a retarded front as evidenced by the location of the 5 ppb isochlor. After the fourteen (14) year phase II simulation period, the 5 ppb isochlor is 15 meters above the water table at the deepest location. In contrast, the 5 ppb isochlor had already reached the water table at all points of the solution domain in Figure 4.4c (where organic carbon fraction equals 1.0 percent).

The following were accomplished to achieve project objectives.

- . Completed literature review of TCE transport
- . Procured and installed FTN 77/386 FORTRAN compiler, with DOS EXTENDER to utilize all available RAM.
- . Procured and installed SWANFLOW on a 386/25 microcomputer, and performed simulations for hypothetical systems.
- . Evaluated the applicability and efficiency of SWANFLOW to NAPL contamination problem at Chempit 4.
- . Determined that SWANFLOW was inappropriate for Chempit 4 problem.
- . Obtained and installed a numerical code, SOILP, for estimating Suction-Water curve (Van-Genuchten) parameters.
- . Procured and installed MOFAT on a 386/25 microcomputer, VAX mainframe, and CRAY supercomputer.
- . Improved computational efficiency by 67% through vectorization and optimization of MOFAT on a CRAY supercomputer.
- . Evaluated the sensitivity of 3-phase flow and chemical transport simulation in MOFAT to discretization in time and space.
- . Determined the optimal time step and mesh size to reduce computational cost without loss of numerical accuracy.

- . Performed numerical simulation to determine the influence of geohydrologic, fluid and transport properties on NAPL-TCE behavior.
- . Performed a "rough" calibration of NAPL migration (lateral and vertical movement) to observed data.
- . Determined that the NAPL would almost stop spreading vertically within about 5 years.
- . Calibrated (roughly) adsorbed TCE concentrations to observed data.
- . Predicted (roughly) that 12 years would be required for soluble TCE to reach the water table.

Analysis of numerical simulations, sensitivity studies, model calibration and future predictions yields the following conclusions.

- i) The nonaqueous phase liquid (NAPL) will be immobilized within the vadose zone, and is not expected to reach the water table.
- ii) Molecular diffusion is the predominant transport mechanism by which soluble TCE will migrate downward through the vadose zone.
- iii) From a worst case perspective, soluble TCE will probably reach the water table within twelve (12) years after infiltration begins. Water containing concentrations of five (5) parts per billion, equal to the drinking water standard of TCE, will reach the groundwater at Chempit 4.
- iv) Improving model calibration and prediction will require data from more soil borings. Predictions will be enhanced by improved data on soil-water-chemical relations.

Better calibration and verification of model predictions are possible if the following recommendations are implemented:

i) Deeper soil borings should be performed and aqueous phase TCE concentrations should be determined, if practical. Better estimates of initial NAPL composition and total volume of disposed NAPL should be provided if they can be obtained.

ii) Future modeling of TCE fate and transport should include other physical, and biochemical processes such as degradation, volatilization and soil evaporation. This will require field and laboratory investigation.

iii) Future 2-D or 3-D simulations should be performed on high performance computers (e.g 486/50 microcomputer, workstation, minicomputer or supercomputer).

iv) A numerical code should be used to formulate and evaluate the effect of remedial options before any potentially costly measures are implemented.

v) Application of venting and vadose zone bioremediation should be considered.

vi) The groundwater at Chempit 4 should be tested for TCE contamination.

ACKNOWLEDGEMENTS

We appreciate the financial support, consideration and advice of Dr. Bob James, Office of Environmental Management, Hill AFB, Utah and Craig Hansen, Gene Wright and Joe Broberg of Engineering Science, INC. We appreciate the wise counsel and generous friendship of Dr. Melvin Campbell, Battelle Northwestern. We appreciate the opportunity to interact with and observe the field methods of Mark Byrnes and others of S.A.I.C.

Abriola, L.M. and G.F. Pinder. 1985. A multiphase approach to the modelling of porous media contamination by organic compounds-1. Equation development. *Water Resources Research* 21(1):11-18.

Abriola, L.M. and G.F. Pinder. 1985. A multiphase approach to the modelling of porous media contamination by organic compounds-2. Numerical simulation. *Water Resources Research* 21(1):19-26.

Allen, M.B. 1985. Numerical modelling of multiphase flow in porous media. *Advances in Water Resources* 8:162-187.

Anand, S.C. and A. Pandit. 1983. A finite element model to predict the flow of underground contaminants due to leakage of chemicals and-or radioactive materials from a buried containment. *Water Resources Research Institute, Clemson University, SC.* 1-258.

Avon, L. and J.D. Bredehoeft. 1989. An analysis of Trichloroethylene movements in groundwater at the Castle Air Force Base, CA. *Journal of Hydrology*, 110:23-50.

Baehr, A.L. 1984. Immiscible contaminant transport in soils with an emphasis on gasoline hydrocarbons, Ph.d. dissertation, Univ. of Delaware, Newark.

Baehr, A.L. 1987. Selective transport of hydrocarbons in the unsaturated zone due to aqueous and vapor phase partitioning, *Water Resour. Res.*, 23(10):1926-1938.

Baehr, A.L. and M.Y. Corapcioglu. 1987. A compositional multiphase model for groundwater contamination by petroleum products, 2, Numerical solution, *Water Resour. Res.*, 23(1):201-213.

Bear, J. 1979. *Hydraulics of groundwater.* McGraw-Hill, New York, NY. 569.

Bear, J., and G. Dagan. 1964. Some exact solutions of interface problems by of the hodograph method. *Journal of Geophysical Research* 69:1563-1572.

Bejan, A. 1984. *Convection Heat Transfer,* John Wiley and Sons, New York.

Buckley, S.E., and M.C. Leverett. 1942. Mechanism of fluid displacement in sands, *Am. Inst. Min. Eng.*, 146:107-116.

Burmester, D.E., and R.H. Harris. 1982. Groundwater Contamination: An Emerging Threat, *Technology Review*, 84(7):50-62.

Byer, H.G., W. Balckenship, and R. Allen. 1990. Groundwater contamination by Chlorinated hydrocarbons: Causes and Prevention.

Civil Engineering, ASCE. 54-55.

Chrichlow, H.B. 1977. Modern Reservoir Engineering - A simulation Approach. Prentice-Hall. Englewood Cliffs, N.J.

Corapcioglu, M.Y., and M.A. Hossain. 198 . Groundwater Contamination by High-Density Immiscible Hydrocarbon Slugs in Gravity-Driven Gravel Aquifers. Groundwater.

Corapcioglu, M.Y., and A. Baehr. 1987. A Compositional Multiphase Model for Groundwater contamination by Petroleum Products, I: Theoretical Considerations. Water Resources Research 23(1):191-200.

Dagan, G., and J. Bear. 1968. Solving the problem of interface upconing in a coastal aquifer by the method of small perturbations. Journal of Hydraulic Research 6(1):15-44.

Dongara, J.J., C.B. Mofer, J.R. Brunch, and G.W. Stewart. 1979. Limpack user's guide. Siam, Philadelphia, P.A.

Dzombak, D.A. and R.G. Luthy. 1984. Estimating adsorption of polycyclic aromatic hydrocarbons on soils. Soil Science. 137(5):292:308.

Eisenberg, M.S., and L.E. Malvern. 1973. On finite element integration in natural coordinates. International Journal for Numerical Methods in Engineering 7:574-575.

Environmental Protection Agency. 1976. Criteria for classification of solid waste disposal facilities and practices. Report SW-821, Prepared by the Office of Solid Waste (WH-564), Washington, D.C.

Environmental Systems & Technologies, Inc. 1990. MOFAT, A two-dimensional finite element program for multiphase flow and multicomponent transport. Program Documentation for Version 2.0. Blacksburg, VA.

Faust, R.F. 1985. Transport of Immiscible Fluids Within and Below the Unsaturated Zone: A Numerical Model. Water Resources Research 21(4):587-596.

Faust, C.R. and J.O. Rumbaugh. 1989. SWANFLOW: Simultaneous Water, Air, and Nonaqueous Phase Flow Version 1.0. Geotrans Inc., VA.

Faust, C.R. 1985. Transport of immiscible fluids within and below the unsaturated zone: A numerical model. Water Resources Research 21(4):587-596.

Freeberg, K.M., P.B. Bedient, and J.A. Connor. 1986. Modeling of TCE Contamination and Recovery in a Shallow Sand Aquifer. Groundwater.

Freeze, R.A., and J.A. Cherry. 1979. Groundwater contamination. In Groundwater, Prentice-Hall, Englewood Cliffs, N.J. 383-462.

Fried, J.J., P. Muntzer, and L. Zilliox. 1979. Ground-water pollution by transfer of oil hydrocarbons. Groundwater 17(6):586-594.

Frind, E.O. 1982. Simulation of long-term transient density-dependent transport in groundwater. Advances in Water Resources. 5:73-88.

Frind, E.O. 1980. Seawater intrusion in continuous coastal aquifer-aquitard systems. In Finite Element in Water Resources, Proceedings of the Third International Conference on Finite Elements in Water Resources, University of Mississippi, University, Mississippi. 2. 177-2.198.

Gray, W.G. and J.L. Hoffman. 1983. A numerical model of groundwater contamination from Price's Landfill, New Jersey - I. Data base and flow simulation. Groundwater 21(1):7-14.

Gray, W.G. and J.L. Hoffman. 1983. A numerical model of groundwater contamination from Price's landfill, New Jersey-II. Sensitivity analysis and contaminant plume simulation. Groundwater 21(1):15-21.

Hantush, M.S. 1968. Unsteady movement of freshwater in thick unconfined saline aquifers. Bulletin of the International Association of Scientific Hydrology 13(2):40-60.

Hassanizadeh, M., and W.G. Gray. 1979a. General conservation equations for multi-phase systems. -1. Averaging procedure. Advances in Water Resources. 2:131-144.

Hassanizadeh, M., and W.G. Gray. 1979b. General conservation equations for multi-phase systems. -2. Mass, momenta, energy, and entropy equations. Advances in Water Resources. 2:191-203.

Hazardous Waste Remediation Actions Program: Martin Marietta Energy Systems, Inc. 1988. U.S. Air Force Installation restoration program: Preliminary assessment/site inspection. Chemical disposal pit no.4 at Utah Test & Training Range/Hill Air Force Base, Utah.

Henry, H.R. 1959. Saltwater intrusion into freshwater aquifers. Journal of Geophysical Research 64:1911-1919.

Henry, H.R. 1964. Effects of dispersion on saltwater encroachment in coastal aquifers, in seawater in coastal aquifers. U.S. Geological Survey Water Supply Paper 1613-C.

Heutmaker, D.L., F.L. Peterson., and S.W. Wheatcraft. 1977. A laboratory study of waste water injection into a Ghyben-Herzberg groundwater system under dynamic conditions. Technical Report No. 107, University of Hawaii, Honolulu, Hawaii.

Hunt, J.R. and N. Sitar. 1988. Nonaqueous phase liquid transport and cleanup -1. Analysis of mechanism. Water Resources Research 24(8):1247-1258.

Huyakorn, P.S., P.F. Anderson, J.W. Mercer, and H.O. White, Jr. 1987. Saltwater intrusion in aquifers: development and testing of a three-dimensional finite element. Model. Water Resources Research 23(2):293-312.

Huyakorn, P.S. and G.F. Pinder. 1978. A new finite element technique for the solution of two-phase flow through porous media. Advances in Water Resources 1(5):285-298.

Huyakorn, P.S. and S.D. Thomas. 1984. Techniques for making finite elements competitive in modeling flow in variably saturated porous media. Water Resources Research 20(8):1099-1115.

Huyakorn, P.S., S.D. Thomas, J.W. Mercer, and H.B. Lester, 1983. SATURN: A finite element model for simulating saturated-unsaturated flow of radionuclide transport, report prepared for Electric Power Research Institute, Geotrans., Herndon, VA.

IRPTC, UN Environmental Program Treatment and Disposal Methods for Waste Chemicals.

Kaluarachchi, J.J. and J.C. Parker. 1988. An efficient finite element method for modeling multiphase flow. Water Resources Research 25(1):43-54.

Kaluarachchi, J.J., Parker, J.C. and Lenhard, R.J., 1990. A numerical model for water and light hydrocarbon migration in unconfined aquifers under vertical equilibrium. Adv. Water Resour. (in press).

Knox, R.C., L.W. Canter, and D.F. Kincannon. 1982. Case studies of aquifer restoration. Presented at the Spring Convention, Am. Soc. Civ. Eng., Las Vegas, Nev., April 26-30.

Konikow, L.F., and J.D. Bredehoeft. 1978. Computer model of two dimensional solute transport and dispersion in groundwater. Techniques of Water Resources Investigations of the U.S. Geological Survey, Book 7, Chapter C.2. U.S. Government Printing Office, Washington.

Kuppusamy, T., J.C. Parker., and R.J. Lenhard. 1987. Finite-element analysis of multiphase immiscible flow through soils. Water Resources Research 23(4):625-631.

Kuppusamy, T., J. Sheng, J.C. Parker, and R.J. Lenhard. 1987. Finite Element Analysis of Multiphase Immiscible Flow Through Soils. Water Resources Research 23(4):625-631.

Lee, C.H. and R.T. Cheng. 1974. On seawater encroachment in coastal aquifers. Water Resources Research 10(5):1039-1043.

Leverett, M.C., and W.B. Lewis. 1941. "Steady flow of gas-oil-water mixtures through unconsolidated sands." Trans. Soc. Pet. Eng. AIME, 142, 107-116.

Leverett, M.C. 1941. "Capillary behavior in porous solids," Trans. Soc. Pet. Eng. AIME, 142, 152-169.

Lin, C., G.F. Pinder, and E.F. Wood. 1982. Water Resources Program Report. 83-WR-2. Water Resources Program, Princeton University, Princeton, N.J.

Mercer, J.W., and C.R. Faust. 1976. The application of finite element techniques to immiscible flow in porous media, in Finite Elements In Water Resources, edited by W.G. Gray, G.F. Pinder, and C.A. Brebbia.:1.21-1.57, Pentech, London.

Mercer, J.W. and C.R. Faust. 1977. The application of finite element techniques to immiscible flow in porous media. Finite Elements in Water Resources: Proceedings of the first international conference on finite elements in water resources held at Princeton University, U.S.A., July 1976. Pentech Press, London.

Mercer, J.W., S.P. Larson, and C.R. Faust. 1980. Simulation of salt-water interface motion. Ground Water 18(4):374-385.

Mull, R. 1971. Migration of oil products in the subsoil with regard to groundwater pollution by oil, in Advances in Water Pollution Research Proceedings of the 5th International Conference, 1970. Pergamon, New York.

Neuman, S.P., R.A. Feddes, and E. Bresler. 1974. Finite Element Simulation of flow in saturated-unsaturated Soils considering water uptake by plants. In Development of Methods, Tools and Solutions for Unsaturated Flow, Third Annual Report (Part 1). Technician Institute of Technology, Haifa, Israel.

Oak Ridge National Laboratory. 1989. The installation restoration program toxicology guide, Vol 1-4. AF Systems Command, Wright Patterson AFB, OH.

Office of Technology Assessment. 1987. Identifying and regulating carcinogens-Background-Paper, Rep. OTA-BP-H-42, U.S. Government Printing Office, Washington, D.C.

Osborne, M. and J. Sykes. 1986. Numerical modeling of immiscible organic transport at the Hyde Park landfill. Water Resources Research 22(1):25-33.

Parker, J.C., R.J. Lenhard, and T. Kuppusamy. 1987. A parametric model for constitutive properties governing multiphase flow in porous media. Water Resources Research 23(4):618-624.

Paschke, N.W. 1982. Mean behavior of buoyant, contaminant plumes in groundwater. M.S. Report, Dept. of Civ. and Environ. Engr., Univ. of Wisc., Madison, WI.

Paschke, N.W., and J.A. Hoopes. 1984. Buoyant contaminant plumes in groundwater. Water Resources Research 20(9):1183-1192.

Peaceman, D.W. 1977. Fundamentals of numerical reservoir simulation. Elsevier Scientific Publishing Co., Amsterdam.

Petrov, A.A., Petroleum Hydrocarbons, Springer-Verlag, New York, 1987.

Pinder, G.F. and L.M. Abriola. 1986. On the Numerical Simulation of Nonaqueous Phase Organic Compounds in the Subsurface. Water Resources Research 22(9): 109S-119S.

Pinder, G.F. and H.H. Cooper, Jr. 1970. A numerical technique for calculating the transient position of the saltwater front. Water Resources Research 6(3):875:880.

Pinder, G.F. and E.O. Frind. 1972. Application of Galerkin's procedure to aquifer analysis. Water Resources Research 8:108.

Pinder, G.F., and R.H. Page. 1977. Finite element simulation of saltwater intrusion on the south fork of Long Island. Proceedings of the 1st International Conference on Finite Elements in Water Resources, Pentech Press, London, p 2.51-2.69.

Quashigah, G.N. 1988. Simulating Density Dependent Transport in Groundwater Aquifers using Physical and Numerical Models. C.E. thesis, Utah State University, Logan, UT.

Redell, D.L. and D.K. Sunada. 1970. Numerical simulation of dispersion in groundwater aquifers. Hydrology Papers no. 41, Colorado State University, Fort Collins, Colorado. p. 79.

Sa'da Costa, A.A. and J.L. Wilson. 1979. Numerical model of seawater intrusion in aquifers. MIT Rep 247, Massachusetts Institute of Technology, Cambridge, Massachusetts.

SAIC, Site Inspection Report for Explosive Ordnance Thermal Treatment Unit and Chemical Disposal Pit No. 4, Oasis-Site, Utah Test Training Range, North Range, Utah, 1990.

Schmorak, S. and A. Mercado. 1969. Upconing of freshwater-seawater interface below pumping wells. Field study, Water Resources Research 5(6):1290-1311.

Schwartz, F.W., J.A. Cherry/., and J.R. Roberts. 1982. A case study of a chemical spill: Polychlorinated Biphenyls (PCBs) -2. Hydrogeological conditions and contaminant migration. Water Resources Research 18(3):535-545.

Schwille, F. 1988. Dense Chlorinated Solvents in Porous and Fractured Media. Lewis Publishers, Chelsea, MI.

Segerlind, L.J. 1984. Applied finite element analysis. John Wiley and Sons, New York, NY.

Segol, G., G.F. Pinder, and W.G. Gray. 1975. A Galerkin finite element technique for calculating the transient position of the saltwater front. Water Resources Research 11(2):343-347.

Segol, G. 1976. A three dimensional Galerkin finite element model for the analysis of contaminant transport in saturated-unsaturated porous media, p. 2.123-2.144. In Proceedings of the First International Conference on Finite Elements in Water Resources, Pentech Press, London.

Shamir, V. and G. Dagan. 1971. Motion of the seawater interface in coastal aquifers: a numerical solution. Water Resources Research 7(3):644-657.

Stone, H.L., 1973. Estimation of 3-phase relative permeability and residual oil data, Journal of Canadian Petroleum Technology 12(4) pp. 53-61.

Taylor C., and P.S. Huyakorn. 1978. Three-dimensional groundwater flow with convective dispersion, p. 311-321. In Finite elements in fluids, Vol. 3, John Wiley and Sons, New York, NY.

Thibodeaux, L.J. 1979. Chemodynamics. John Wiley & Sons, New York.

U.S. EPA. 1980. National Conference on Management of Uncontrolled Hazardous Waste Sites, Oct. 15-17, 1980, Washington, D.C.

U.S. EPA. 1981. Management of Uncontrolled Hazardous Waste Sites, National Conference On, Oct. 15-17, Washington, D.C.

Van Dam, J. 1967. The migration of hydrocarbons in a water bearing stratum, in The Joint Problems of the Oil and Water Industries, edited by P. Hepple. Elsevier. New York.

Villaume, J.F. 1985. Investigations at Sites Contaminated with dense Nonaqueous phase liquids (NAPL). Groundwater Monitoring Review. 5(2):60-74.

Van Genutchen, R. "Calculating the unsaturated hydraulic conductivity with a new, closed-form analytical model. Research Report 78-WR-08. Water Resources Program, Dept. of Civil Engineering, Princeton University, Princeton, N.J.

Van Genutchen, M.T., "A closed-form equation for predictions, the hydraulic conductivity of unsaturated soils." Soil Science Society of American Journal, 44 892-898, 1980

Vemuri, V., and W.J. Karplus, Digital Computer Treatment of Partial Differential Equations, Prentice Hall, Inc., Englewood Cliffs, New Jersey, 1981.

Voss, C.I. 1984. A finite element simulation model for saturated-unsaturated fluid-density dependent groundwater flow with energy transport or chemically reactive single species solute transport. U.S. Geological Survey, National Center, Reston, Virginia. pp. 1-220.

Waite, D.A., Preclosure Radiological Calculations to Support Salt Site Evaluations, Technical Report Prepared for Office of Nuclear Waste Isolation, Columbus, OH, 1984.

Wirojanagud, P. and R.J. Charbeneau. 1985. Saltwater upconing in unconfined aquifers. Journal of Hydraulics Engineering, American Society of Civil Engineers 111(3):417-434.

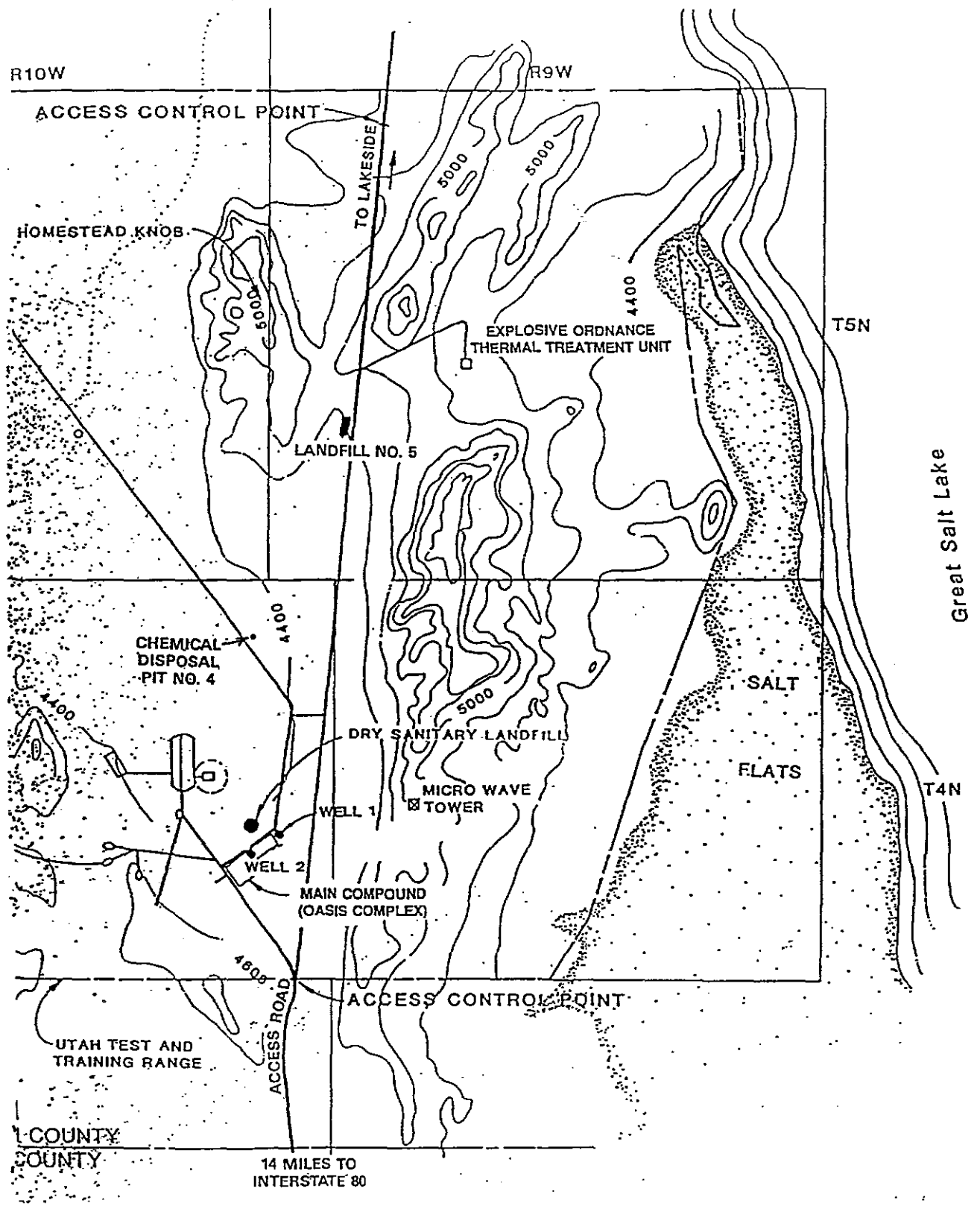
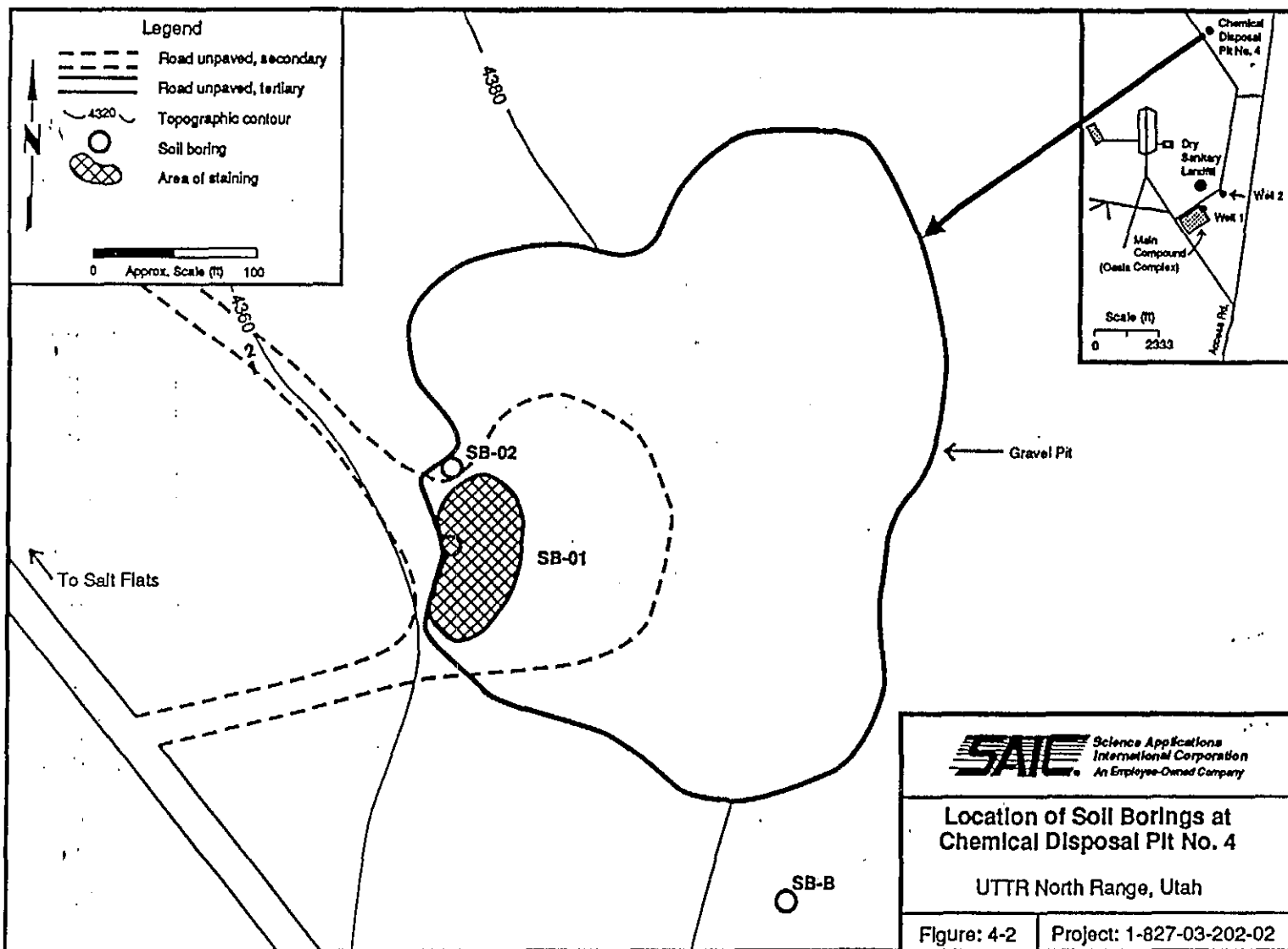


Figure 1.2 Location of Chempit 4 at the UTR North Range, Utah (SAIC 1990, p.2:3)



Note: Locations of data points and outline of pit have not been surveyed.

Source: U.S.G.S. Sally Mountain, Utah, Topographic Quadrangle.

Figure 1.3 Areal extent of Chemical Contamination of Chempit 4
(SAIC, August, 1990)

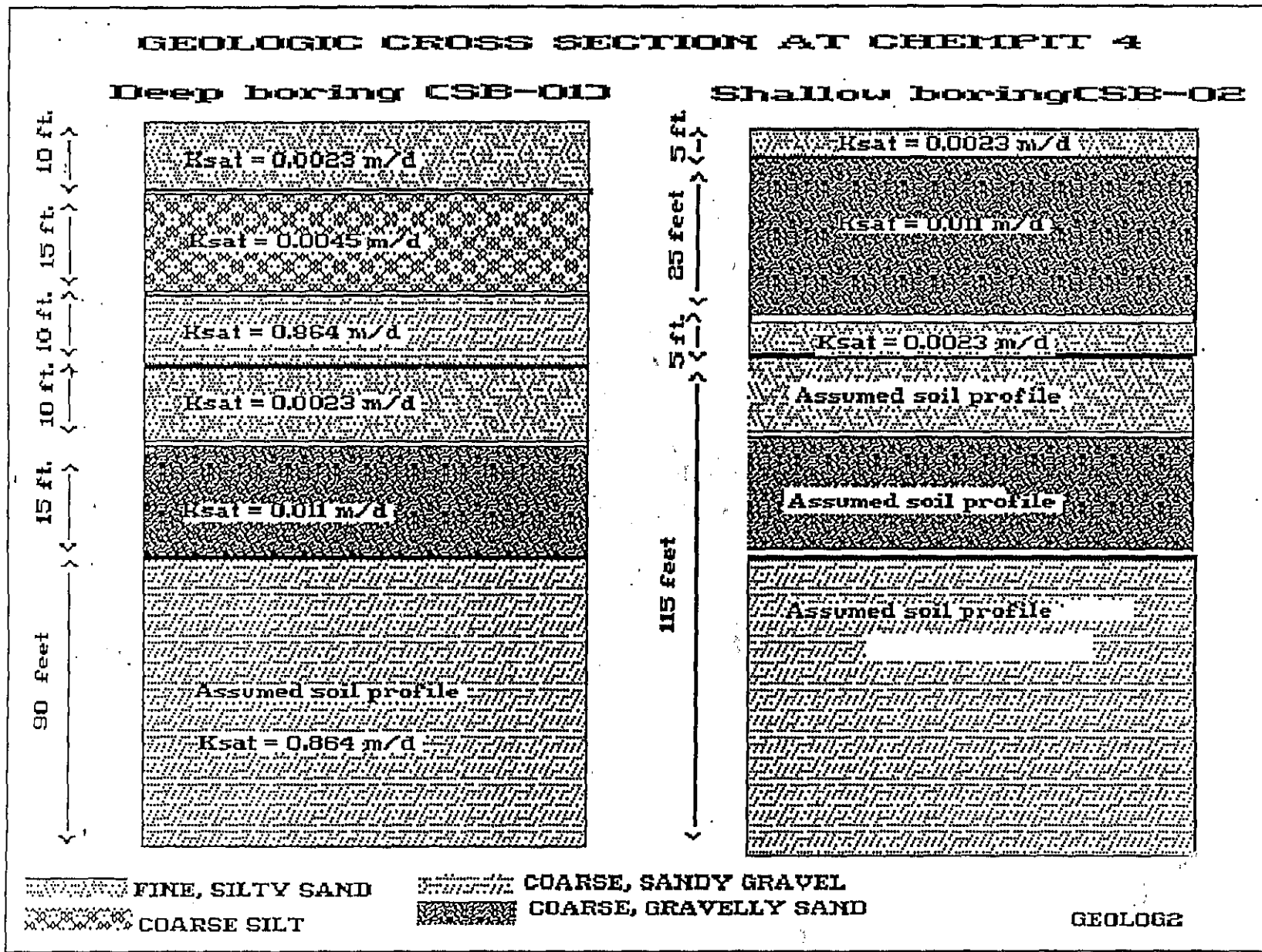
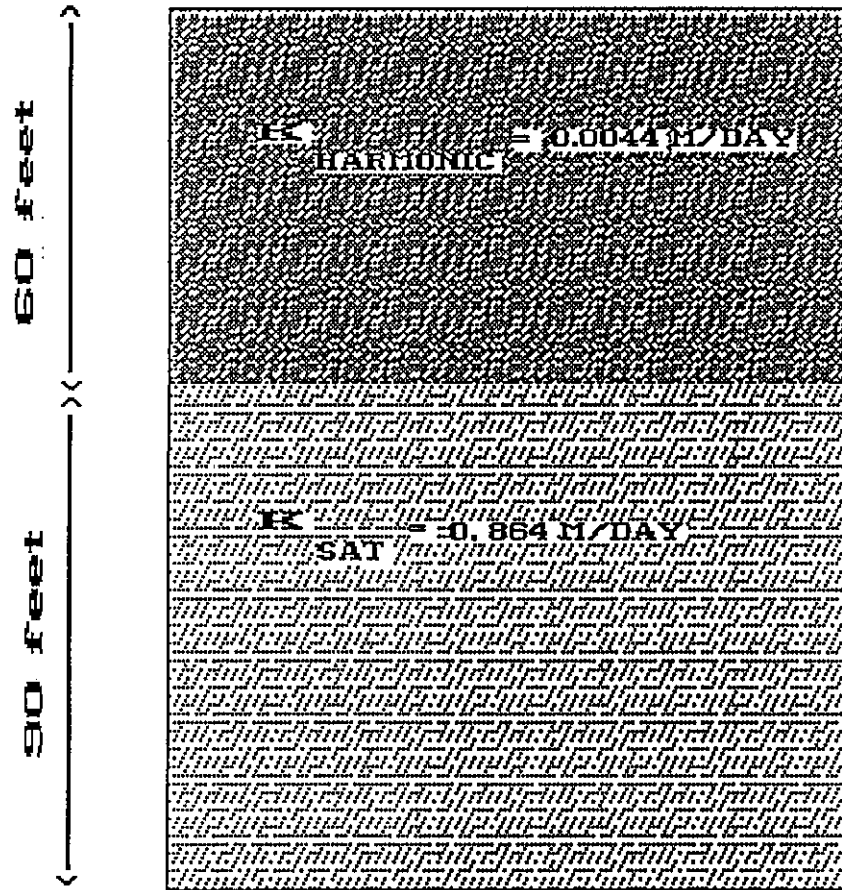


Figure 2.1.1a Actual geologic cross section at Chempit 4

CONCEPTUAL MODEL GEOLOGIC CROSS SECTION

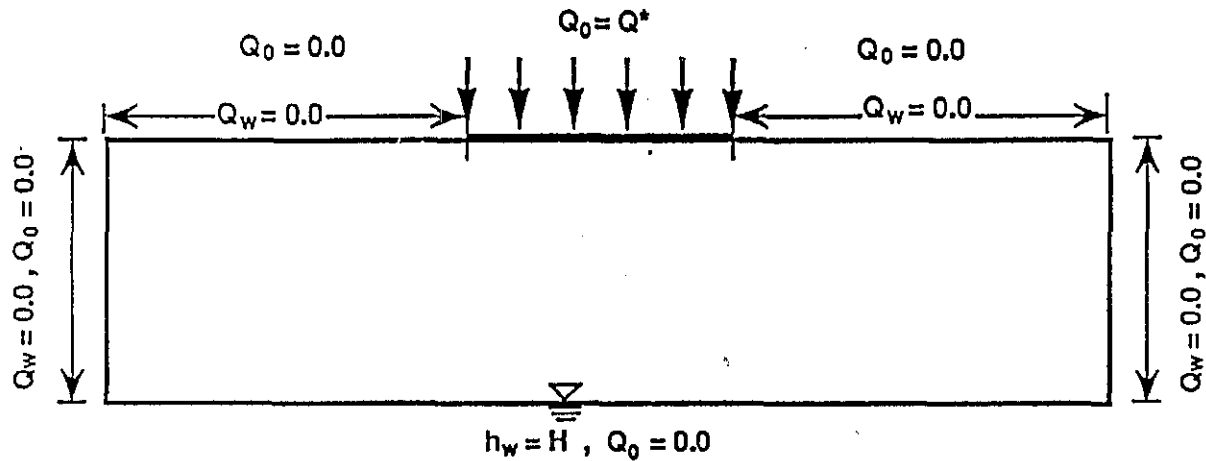


GEOLOG3

Figure 2.1.1b Cross-section of idealized geology of Chempit 4 used for modelling

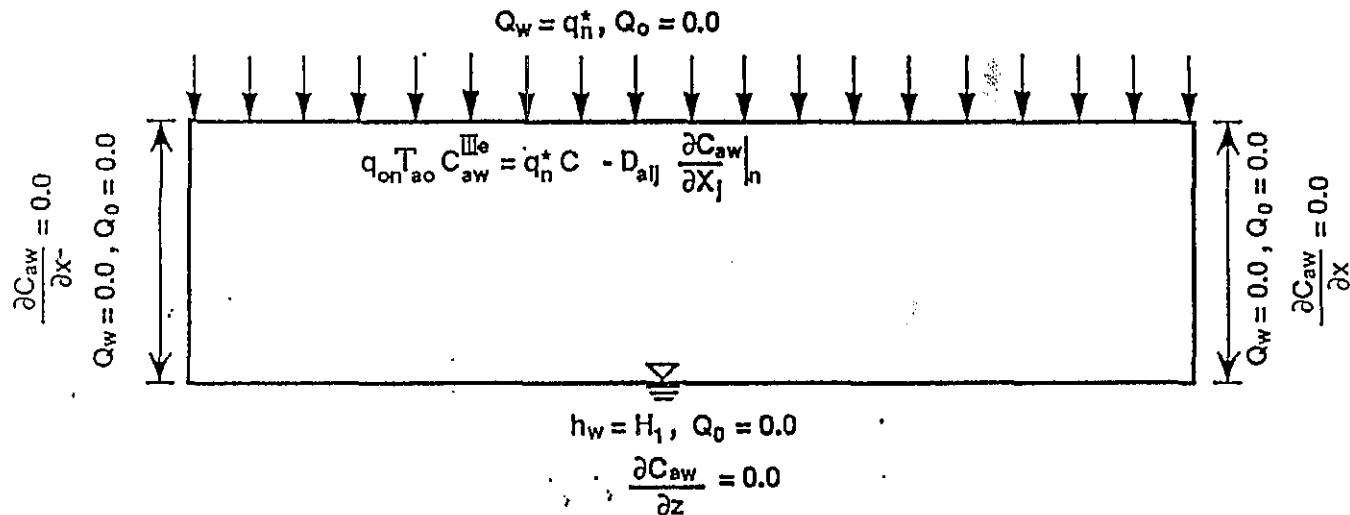
Problem Description and Boundary Conditions

Phase I: Oil-TCE Mixture Infiltration (2 year simulation)



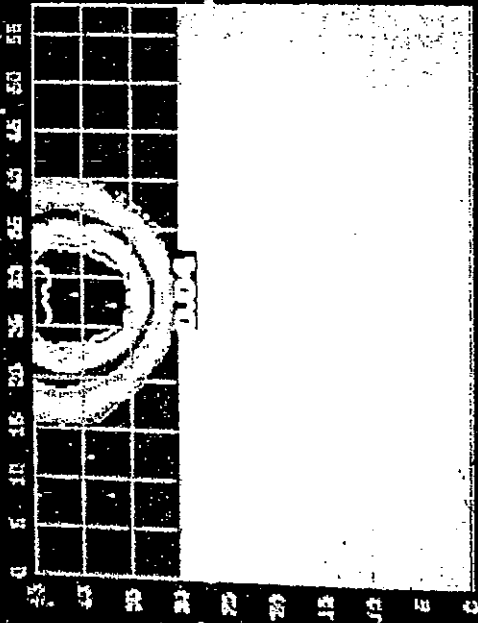
4.1a Problem description and boundary conditions: Oil-TCE mixture infiltration phase (phase I)

Phase II: NAPL Redistribution and Transport (Simulation period > 15 years)

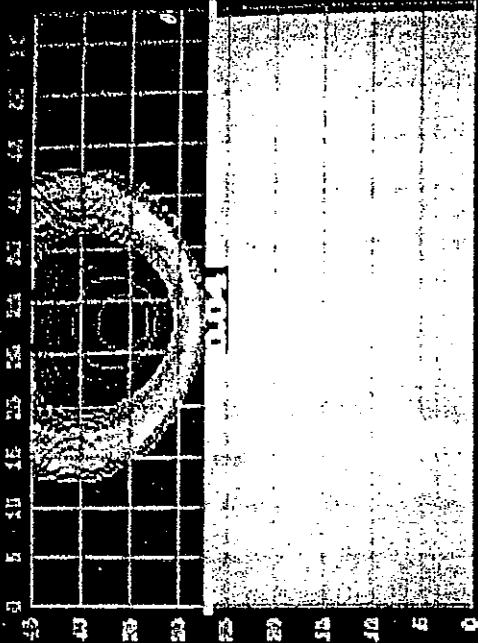


4.1b Problem description and boundary conditions: NAPL redistribution and partitionable TCE transport phase (phase II)

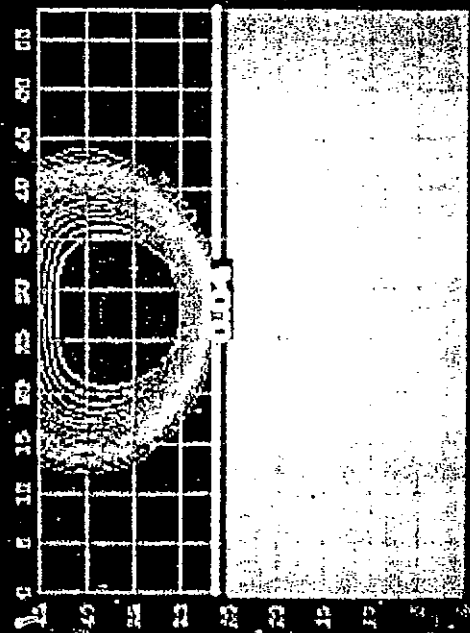
**NAPL SATURATION CONTOURS C-3
 C PHASE II SIMULATIONS: OIL REDISTRIBUTION: NAPL VOLUME = 250,000 GALS.**



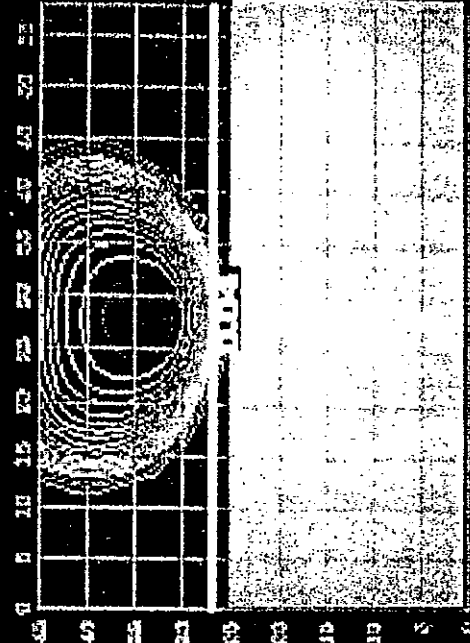
TIME = 0.0 YEARS



TIME = 5.0 YEARS



TIME = 10.0 YEARS



TIME = 14.0 YEARS

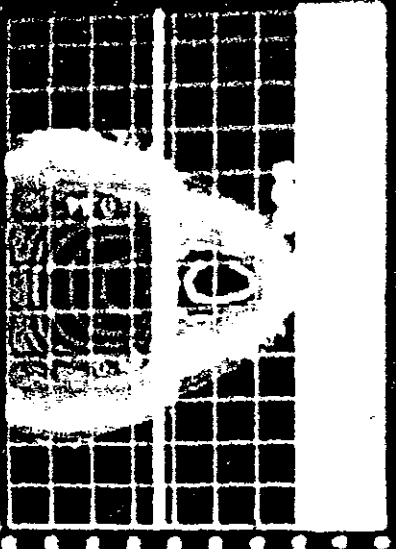
2000000

Figure 4.3.1a NAPL Saturation
 Contours: (Input NAPL volume
 equals 250,000 gallons)

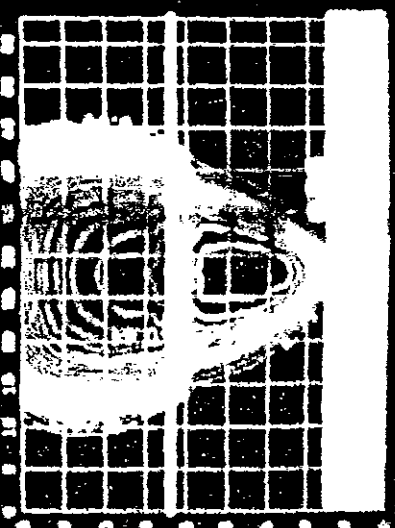
NAPL SATURATION TRENDS CONTINGENCY C-3
C-3: 1980-1985



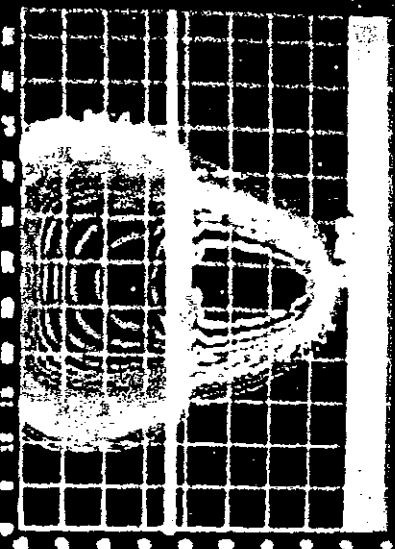
TIME = 0.0 YEARS



TIME = 10.0 YEARS



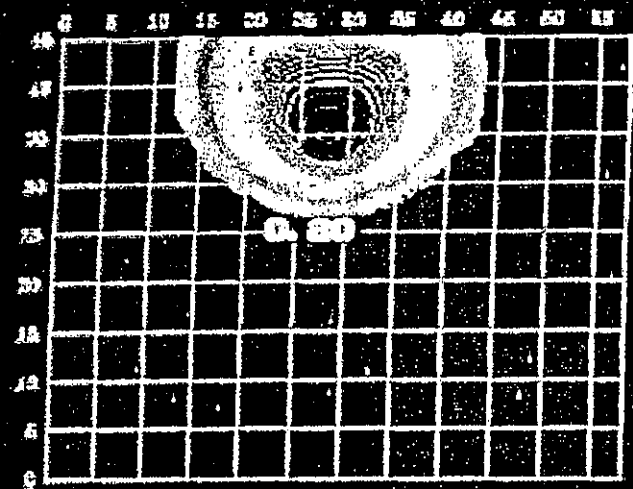
TIME = 20.0 YEARS



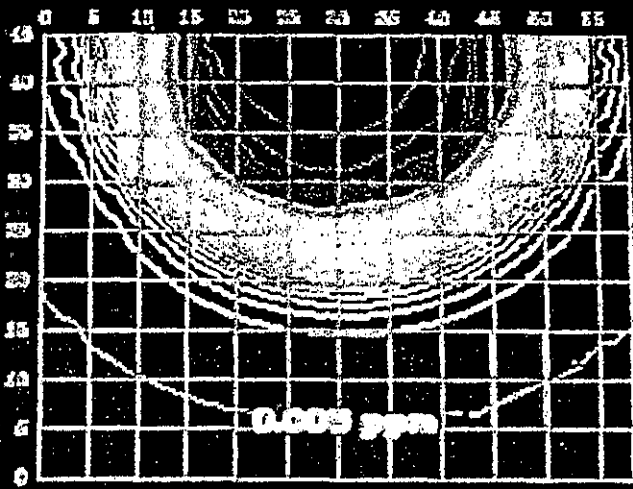
TIME = 30.0 YEARS

Figure 4.3.1b NAPL Saturation
Contours: (Input NAPL volume
equals 500,000 gallons)

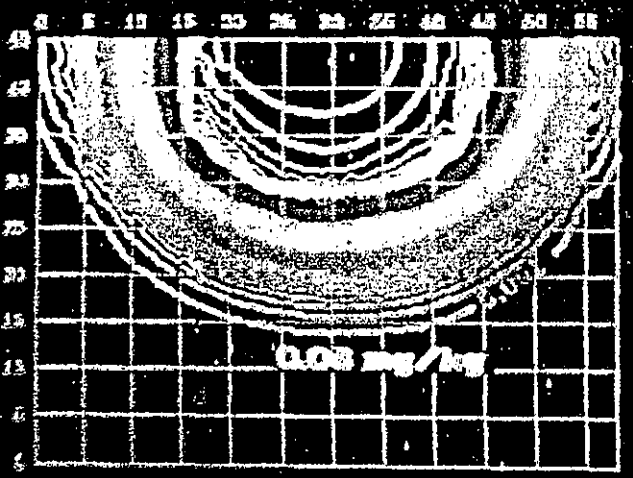
P-PHASE CONCENTRATION DISTRIBUTION OF TCE (TIME = 5 YEARS)



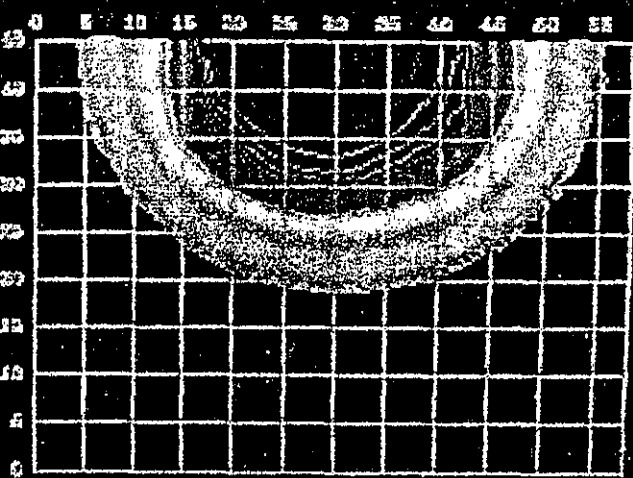
NAPL SATURATION CONTOURS (C-3)



WATER PHASE CONCENT. (CPM)



SOIL PHASE CONCENT. (MG/KG)



GAS PHASE CONCENT. (CPM)

SECRET

NapL Saturation

| |
|-------------|
| 0.20 - 0.25 |
| 0.15 - 0.20 |
| 0.10 - 0.15 |
| 0.05 - 0.10 |
| < 0.05 |

Water phase conc.

| |
|-------------|
| 25 - 32 ppm |
| 21 - 25 ppm |
| 15 - 21 ppm |
| 11 - 15 ppm |
| 2 - 11 ppm |
| < 1.00 ppm |

Soil phase conc.

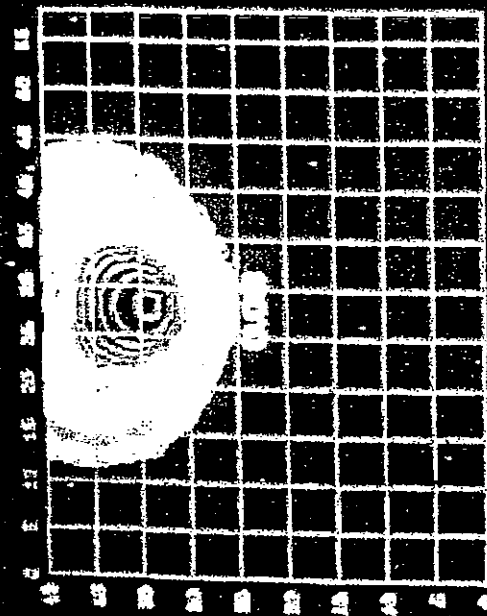
| |
|---------------|
| 37 - 56 mg/kg |
| 35 - 42 mg/kg |
| 19 - 23 mg/kg |
| 13 - 19 mg/kg |
| 5 - 12 mg/kg |
| 0.6 - 5 mg/kg |

Gas phase conc.

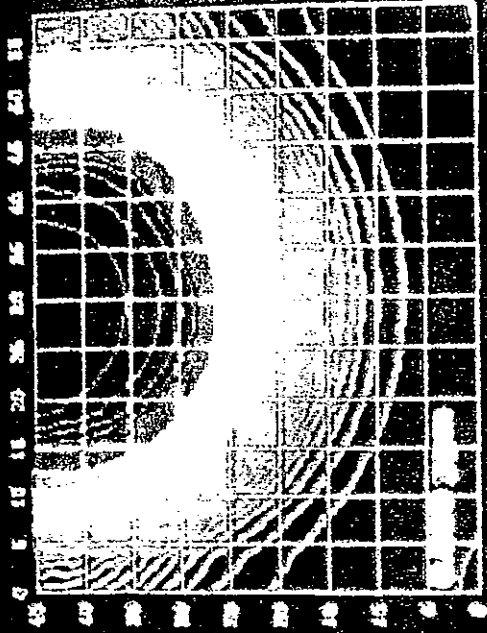
| |
|---------------|
| 11 - 15 ppm |
| 7.5 - 9 ppm |
| 6.3 - 7.5 ppm |
| 4.5 - 6.3 ppm |
| 3.1 - 4.5 ppm |
| 2.0 - 3.1 ppm |

Figure 4.4a P-phase concentration distribution of TCE after 5 years of phase II

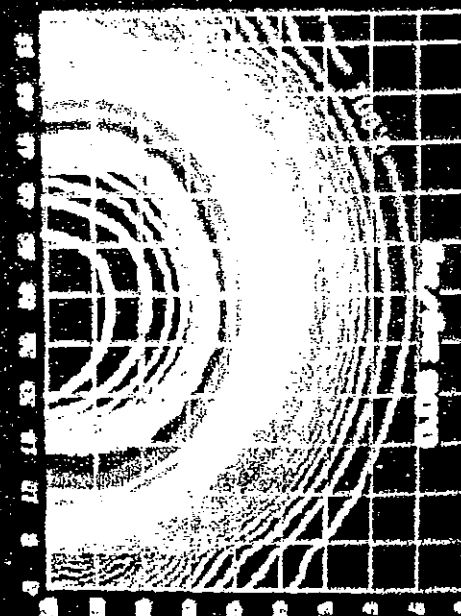
P-PHASE CONCENTRATION DISTRIBUTION OF TCE CUMUL = 10 YEARS



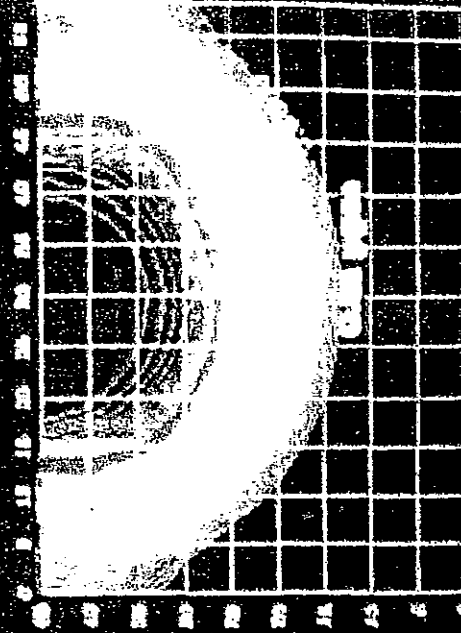
WATER PHASE CONCENT. CUMUL = 10



SOIL PHASE CONCENT. CUMUL = 10



GAS PHASE CONCENT. CUMUL = 10



SOIL PHASE CONCENT. CUMUL = 10

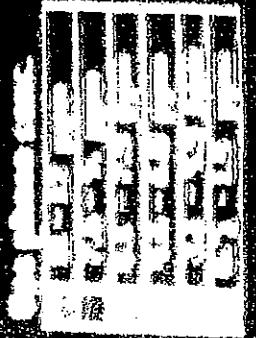
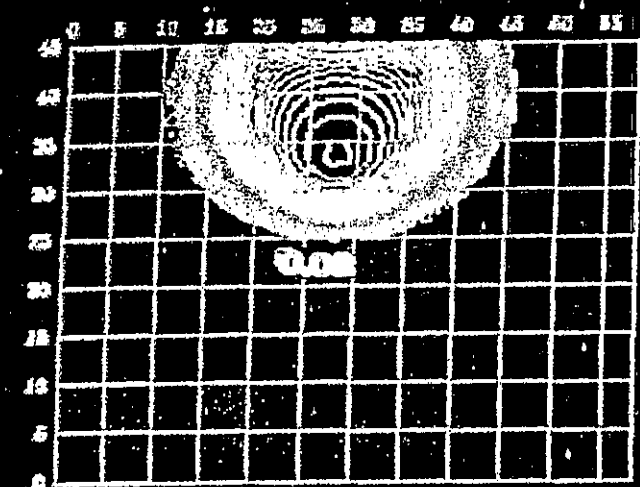
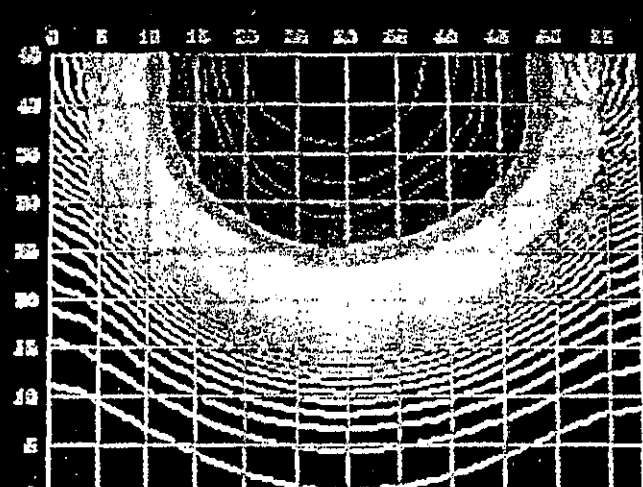


Figure 4.4b P-phase concentration distribution of TCE after 10 years of phase II.

P-PHASE CONCENTRATION DISTRIBUTION OF TCE CTIME = 14 YEARS



NAPL SATURATION CONTOURS C-3



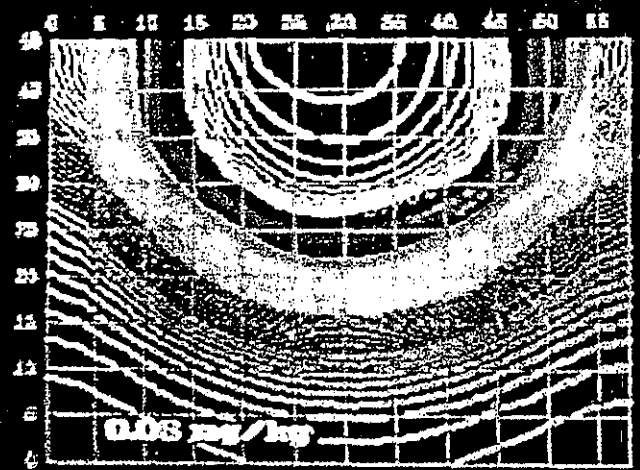
WATER PHASE CONCENT. CPPH3

Napl Saturation

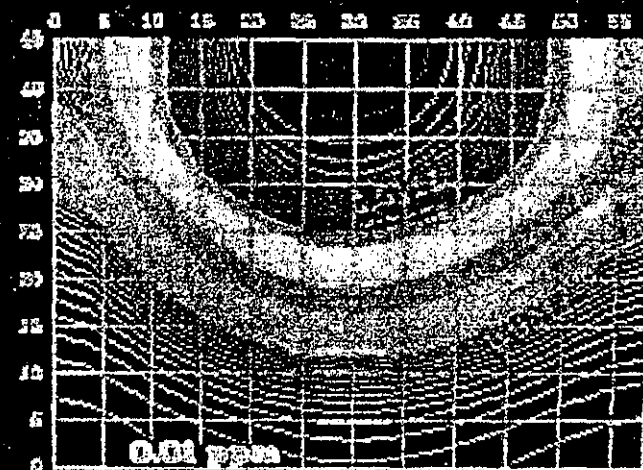
| |
|-------------|
| 0.70 - 0.79 |
| 0.50 - 0.59 |
| 0.20 - 0.29 |
| 0.10 - 0.19 |
| < 0.05 |

Water phase conc.

| |
|-------------|
| 25 - 32 ppm |
| 21 - 25 ppm |
| 15 - 20 ppm |
| 11 - 15 ppm |
| 2 - 10 ppm |
| < 1.00 ppm |



SOIL PHASE CONCENT. CPH3/K03



GAS PHASE CONCENT. CPPH3

Soil phase conc.

| |
|---------------|
| 51 - 55 mg/kg |
| 36 - 52 mg/kg |
| 19 - 24 mg/kg |
| 13 - 17 mg/kg |
| 6 - 12 mg/kg |
| 0.6 - 5 mg/kg |

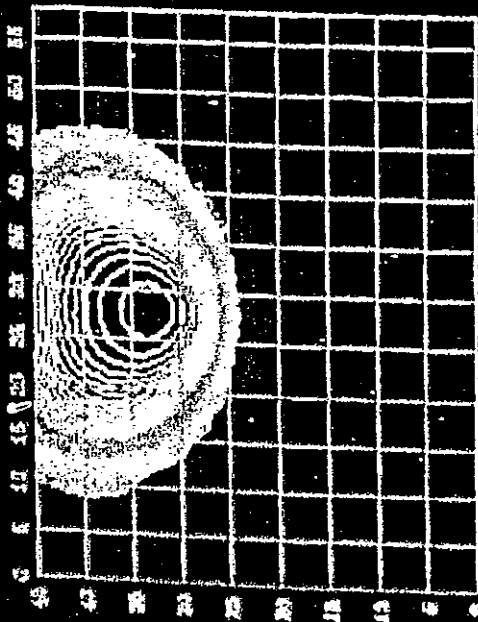
Gas phase conc.

| |
|---------------|
| 11 - 12 ppm |
| 7.5 - 9 ppm |
| 6.2 - 7.5 ppm |
| 4.5 - 6.0 ppm |
| 3.1 - 4.5 ppm |
| 0.8 - 1.5 ppm |

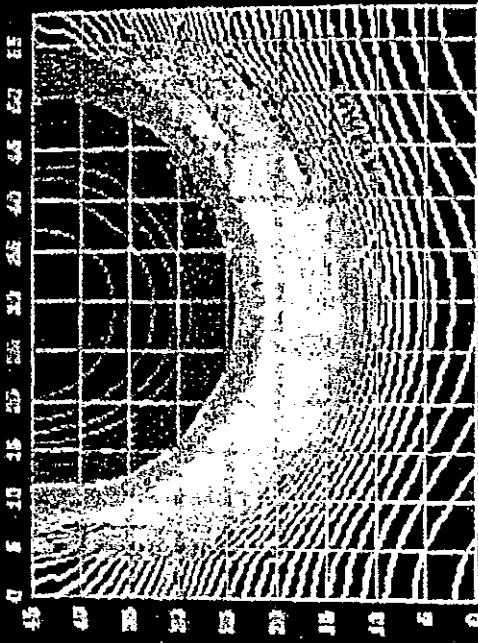
14RCHEAT

Figure 4.4c P-phase concentration distribution of TCE after 14 years of phase II

P-PHASE CONCENTRATION DISTRIBUTION OF TCE CTIME = 25 YEARS



WATER PHASE CONCENT. CPPND



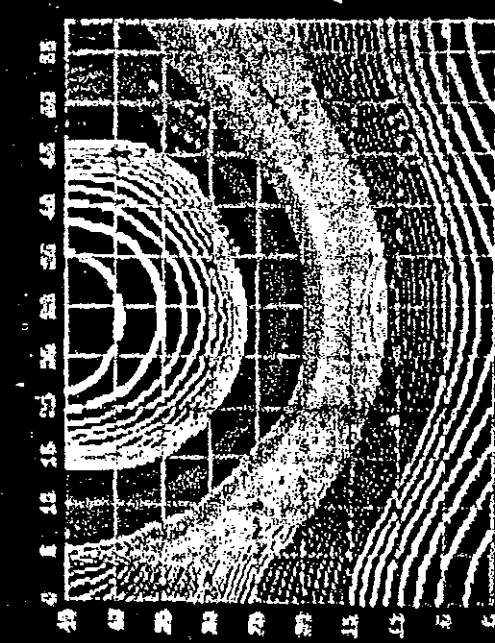
WATER PHASE CONCENT. CPPND

Head Sat. Conc.

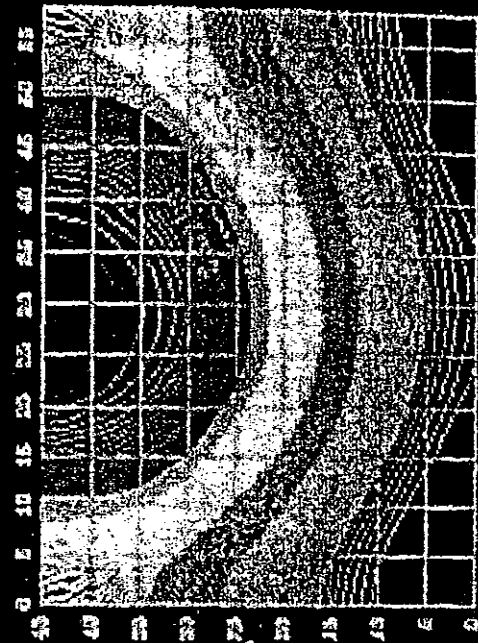
| |
|-------------|
| 0.18 - 0.19 |
| 0.19 - 0.20 |
| 0.20 - 0.21 |
| 0.21 - 0.22 |
| 0.22 - 0.23 |
| 0.23 - 0.24 |
| 0.24 - 0.25 |
| 0.25 - 0.26 |
| 0.26 - 0.27 |
| 0.27 - 0.28 |
| 0.28 - 0.29 |
| 0.29 - 0.30 |
| 0.30 - 0.31 |
| 0.31 - 0.32 |
| 0.32 - 0.33 |
| 0.33 - 0.34 |
| 0.34 - 0.35 |
| 0.35 - 0.36 |
| 0.36 - 0.37 |
| 0.37 - 0.38 |
| 0.38 - 0.39 |
| 0.39 - 0.40 |
| 0.40 - 0.41 |
| 0.41 - 0.42 |
| 0.42 - 0.43 |
| 0.43 - 0.44 |
| 0.44 - 0.45 |
| 0.45 - 0.46 |
| 0.46 - 0.47 |
| 0.47 - 0.48 |
| 0.48 - 0.49 |
| 0.49 - 0.50 |
| 0.50 - 0.51 |
| 0.51 - 0.52 |
| 0.52 - 0.53 |
| 0.53 - 0.54 |
| 0.54 - 0.55 |
| 0.55 - 0.56 |
| 0.56 - 0.57 |
| 0.57 - 0.58 |
| 0.58 - 0.59 |
| 0.59 - 0.60 |
| 0.60 - 0.61 |
| 0.61 - 0.62 |
| 0.62 - 0.63 |
| 0.63 - 0.64 |
| 0.64 - 0.65 |
| 0.65 - 0.66 |
| 0.66 - 0.67 |
| 0.67 - 0.68 |
| 0.68 - 0.69 |
| 0.69 - 0.70 |
| 0.70 - 0.71 |
| 0.71 - 0.72 |
| 0.72 - 0.73 |
| 0.73 - 0.74 |
| 0.74 - 0.75 |
| 0.75 - 0.76 |
| 0.76 - 0.77 |
| 0.77 - 0.78 |
| 0.78 - 0.79 |
| 0.79 - 0.80 |
| 0.80 - 0.81 |
| 0.81 - 0.82 |
| 0.82 - 0.83 |
| 0.83 - 0.84 |
| 0.84 - 0.85 |
| 0.85 - 0.86 |
| 0.86 - 0.87 |
| 0.87 - 0.88 |
| 0.88 - 0.89 |
| 0.89 - 0.90 |
| 0.90 - 0.91 |
| 0.91 - 0.92 |
| 0.92 - 0.93 |
| 0.93 - 0.94 |
| 0.94 - 0.95 |
| 0.95 - 0.96 |
| 0.96 - 0.97 |
| 0.97 - 0.98 |
| 0.98 - 0.99 |
| 0.99 - 1.00 |

Water phase conc.

| |
|--------------|
| 26 - 32 ppm |
| 21 - 25 ppm |
| 16 - 20 ppm |
| 11 - 15 ppm |
| 6 - 10 ppm |
| 1 - 5 ppm |
| 0 - 1.00 ppm |



SOIL PHASE CONCENT. CMC/100



GAS PHASE CONCENT. CPPND

Soil phase conc.

| |
|----------------|
| 31 - 36 mg/kg |
| 26 - 32 mg/kg |
| 21 - 27 mg/kg |
| 16 - 23 mg/kg |
| 11 - 18 mg/kg |
| 6 - 12 mg/kg |
| 1 - 5 mg/kg |
| 0 - 1.00 mg/kg |

Gas phase conc.

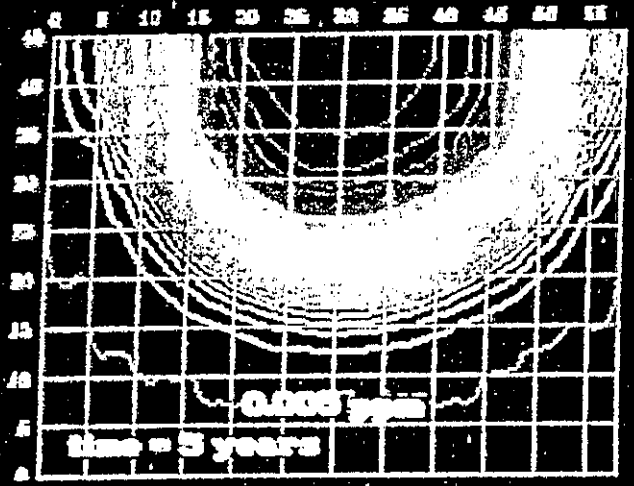
| |
|---------------|
| 11 - 12 ppm |
| 7.6 - 9.1 ppm |
| 5.1 - 7.5 ppm |
| 2.6 - 6.0 ppm |
| 0.1 - 4.5 ppm |
| 0.0 - 1.5 ppm |

SECRET

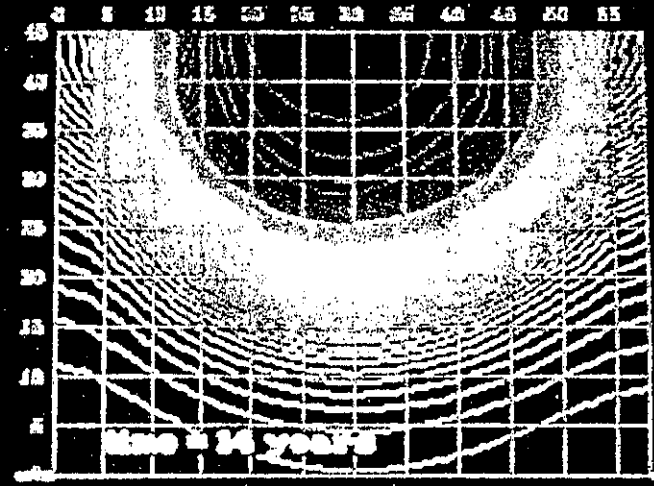
Figure 4.4d P-phase concentration distribution of TCE after 25 years of phase II

EFFECT OF DISPERSIVITY ON TCE TRANSPORT

$P_{\text{con}} = 1.0$ $\alpha_L = \alpha_T = 4.0$



WATER PHASE CONCENT. (PPM)

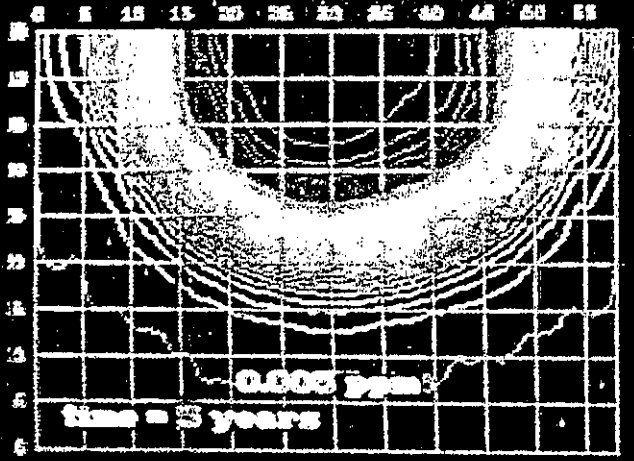


WATER PHASE CONCENT. (PPM)

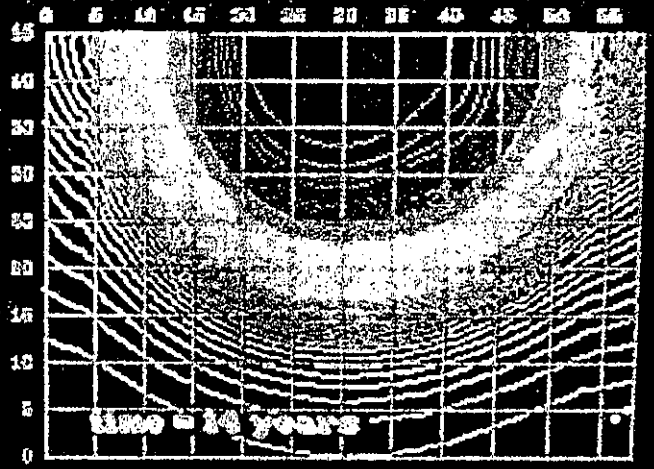
Water phase conc.

| |
|-------------|
| 26 - 32 ppm |
| 21 - 25 ppm |
| 16 - 20 ppm |
| 11 - 15 ppm |
| 6 - 10 ppm |
| 0 - 5 ppm |

$P_{\text{con}} = 2.0$ $\alpha_L = \alpha_T = 2.0$



WATER PHASE CONCENT. (PPM)



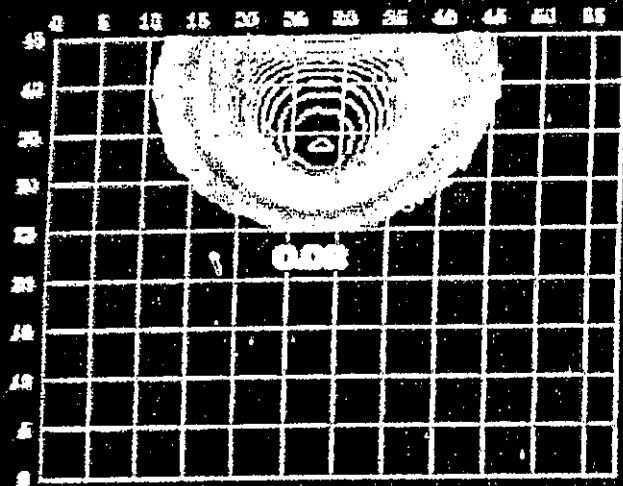
WATER PHASE CONCENT. (PPM)

PECLAT

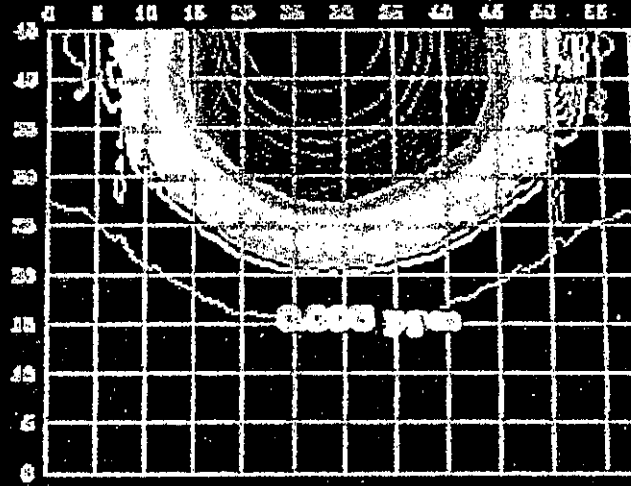
Figure 4.4.1 Effect of dispersivity on water phase TCE concentration after 5 and 14 years of phase II

EFFECT OF ADSORPTION ON TCE TRANSPORT

Organic carbon fraction = 10 %



NAPL SATURATION CONTOURS C-2



WATER PHASE CONCENT. (Cp1) (PPM)

NapL Saturation

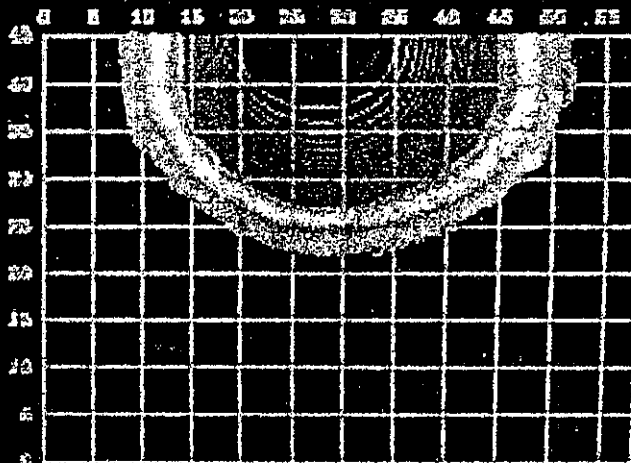
| |
|-------------|
| 0.90 - 0.99 |
| 0.50 - 0.89 |
| 0.20 - 0.49 |
| 0.10 - 0.19 |
| 0.05 |

Water phase conc.

| |
|--------------|
| 25 - 32 ppm |
| 21 - 25 ppm |
| 15 - 20 ppm |
| 11 - 15 ppm |
| 7 - 10 ppm |
| 0 - 1.00 ppm |



SOIL PHASE CONCENT. (Cmg/kg)



GAS PHASE CONCENT. (Cp2) (PPM)

Soil phase conc.

| |
|-----------------|
| 500 - 550 mg/kg |
| 350 - 500 mg/kg |
| 200 - 350 mg/kg |
| 100 - 200 mg/kg |
| 50 - 100 mg/kg |
| 0 - 50 mg/kg |

Gas phase conc.

| |
|---------------|
| 11 - 12 ppm |
| 7.5 - 9 ppm |
| 6.1 - 7.5 ppm |
| 4.5 - 6.0 ppm |
| 3.1 - 4.5 ppm |
| 1.0 - 1.5 ppm |

140C10P

Figure 4.4.2 Effect of adsorption on TCE concentrations after 14 years of phase II